

## Basic Study

**Prolonged high-fat-diet feeding promotes non-alcoholic fatty liver disease and alters gut microbiota in mice**

Kandy T Velázquez, Reilly T Enos, Jackie E Bader, Alexander T Sougiannis, Meredith S Carson, Ioulia Chatzistamou, James A Carson, Prakash S Nagarkatti, Mitzi Nagarkatti, E Angela Murphy

**ORCID number:** Kandy T Velázquez (0000-0003-2427-165X); Reilly T Enos (0000-0001-5571-4586); Jackie E Bader (0000-0002-8383-7898); Alexander T Sougiannis (0000-0002-8512-7291); Meredith S Carson (0000-0002-2186-0195); Ioulia Chatzistamou (0000-0002-6632-8469); James A Carson (0000-0003-3733-8796); Prakash S Nagarkatti (0000-0003-2663-0759); Mitzi Nagarkatti (0000-0002-5977-5615); E Angela Murphy (0000-0002-4803-5822).

**Author contributions:** Velázquez KT performed the majority of experiments and analyzed the data; Chatzistamou I performed histopathological analysis; Velázquez KT performed staining; Velázquez KT, Enos RT, Carson MS, and Sougiannis AT performed molecular investigations; Velázquez KT, Bader JE, Nagarkatti PS, Nagarkatti M and Murphy EA designed and coordinated the microbiome research; Velázquez KT, Enos RT, Carson JA and Murphy EA designed and coordinated the obesity and non-alcoholic fatty liver disease research; Velázquez KT, Enos RT, and Murphy EA wrote the paper; all authors were involved in editing the manuscript.

**Supported by** National Institute of Health, No. NCI-3R01CA121249-08S1, NCCIH-K99AT009206 and No. NCI-1R21CA191966.

**Institutional animal care and use committee statement:** All procedures involving animals were reviewed and approved by the

**Kandy T Velázquez, Reilly T Enos, Jackie E Bader, Alexander T Sougiannis, Meredith S Carson, Ioulia Chatzistamou, James A Carson, Prakash S Nagarkatti, Mitzi Nagarkatti, E Angela Murphy,** Department of Pathology, Microbiology and Immunology, School of Medicine, University of South Carolina, Columbia, SC 29209, United States

**James A Carson,** College of Health Professions, University of Tennessee Health Sciences Center, Memphis, TN 38163, United States

**Corresponding author:** E Angela Murphy, PhD, Associate Professor, Department of Pathology, Microbiology and Immunology, School of Medicine, University of South Carolina, 6439 Garners Ferry Rd, Columbia, SC 29209, United States. [angela.murphy@uscmed.sc.edu](mailto:angela.murphy@uscmed.sc.edu)

**Telephone:** +1-803-2163414

**Fax:** +1-803-2163414

**Abstract****BACKGROUND**

Non-alcoholic fatty liver disease (NAFLD) has become an epidemic largely due to the worldwide increase in obesity. While lifestyle modifications and pharmacotherapies have been used to alleviate NAFLD, successful treatment options are limited. One of the main barriers to finding safe and effective drugs for long-term use in NAFLD is the fast initiation and progression of disease in the available preclinical models. Therefore, we are in need of preclinical models that (1) mimic the human manifestation of NAFLD and (2) have a longer progression time to allow for the design of superior treatments.

**AIM**

To characterize a model of prolonged high-fat diet (HFD) feeding for investigation of the long-term progression of NAFLD.

**METHODS**

In this study, we utilized prolonged HFD feeding to examine NAFLD features in C57BL/6 male mice. We fed mice with a HFD (60% fat, 20% protein, and 20% carbohydrate) for 80 wk to promote obesity (Old-HFD group,  $n = 18$ ). A low-fat diet (LFD) (14% fat, 32% protein, and 54% carbohydrate) was administered for the same duration to age-matched mice (Old-LFD group,  $n = 15$ ). An additional group of mice was maintained on the LFD (Young-LFD,  $n = 20$ ) for a shorter duration (6 wk) to distinguish between age-dependent and age-independent effects. Liver, colon, adipose tissue, and feces were collected for histological and molecular assessments.

Institutional Animal Care and Use Committee at the University of South Carolina.

**Conflict-of-interest statement:** The authors declare no conflicts of interest.

**Data sharing statement:** Data from this manuscript will be available upon request.

**ARRIVE guidelines statement:** The authors have read the ARRIVE guidelines, and the manuscript was prepared and revised according to the ARRIVE guidelines.

**Open-Access:** This article is an open-access article which was selected by an in-house editor and fully peer-reviewed by external reviewers. It is distributed in accordance with the Creative Commons Attribution Non Commercial (CC BY-NC 4.0) license, which permits others to distribute, remix, adapt, build upon this work non-commercially, and license their derivative works on different terms, provided the original work is properly cited and the use is non-commercial. See: <http://creativecommons.org/licenses/by-nc/4.0/>

**Manuscript source:** Unsolicited Manuscript

**Received:** March 7, 2019

**Peer-review started:** March 11, 2019

**First decision:** April 11, 2019

**Revised:** July 5, 2019

**Accepted:** July 16, 2019

**Article in press:** July 17, 2019

**Published online:** August 27, 2019

**P-Reviewer:** Bridle KR, Luo G

**S-Editor:** Cui LJ

**L-Editor:** A

**E-Editor:** Ma YJ



## RESULTS

Prolonged HFD feeding led to obesity and insulin resistance. Histological analysis in the liver of HFD mice demonstrated steatosis, cell injury, portal and lobular inflammation and fibrosis. In addition, molecular analysis for markers of endoplasmic reticulum stress established that the liver tissue of HFD mice have increased phosphorylated Jnk and CHOP. Lastly, we evaluated the gut microbial composition of Old-LFD and Old-HFD. We observed that prolonged HFD feeding in mice increased the relative abundance of the *Firmicutes* phylum. At the genus level, we observed a significant increase in the abundance of *Adercreutzia*, *Coprococcus*, *Dorea*, and *Ruminococcus* and decreased relative abundance of *Turicibacter* and *Anaeroplasma* in HFD mice.

## CONCLUSION

Overall, these data suggest that chronic HFD consumption in mice can mimic pathophysiological and some microbial events observed in NAFLD patients.

**Key words:** High-fat diet; Obesity; Non-alcoholic fatty liver disease; Gut microbiome; Endoplasmic reticulum stress; Inflammation; Fibrosis

©The Author(s) 2019. Published by Baishideng Publishing Group Inc. All rights reserved.

**Core tip:** This work describes how mice consuming a chronic high-fat diet can mimic the clinical characteristics of non-alcoholic fatty liver disease. We used histopathological, metabolic, and molecular approaches to establish that prolonged high-fat-diet feedings in mice may be used as a pre-clinical model to study long-term interventions involving steatosis, steatohepatitis, fibrosis, glucose disturbances, endoplasmic reticulum stress, and gut microbial dysbiosis.

**Citation:** Velázquez KT, Enos RT, Bader JE, Sougiannis AT, Carson MS, Chatzistamou I, Carson JA, Nagarkatti PS, Nagarkatti M, Murphy EA. Prolonged high-fat-diet feeding promotes non-alcoholic fatty liver disease and alters gut microbiota in mice. *World J Hepatol* 2019; 11(8): 619-637

**URL:** <https://www.wjnet.com/1948-5182/full/v11/i8/619.htm>

**DOI:** <https://dx.doi.org/10.4254/wjh.v11.i8.619>

## INTRODUCTION

Advanced stages of non-alcoholic fatty liver disease (NAFLD) can be classified as a form of chronic hepatitis. An estimated 25% of individuals are affected globally<sup>[1]</sup>. In the United States alone, approximately 95 million adults have NAFLD and the prevalence has continued to rise<sup>[2]</sup>. In fact, it is now considered the most common cause of liver disorder in the United States and other Western industrialized countries. NAFLD exists as a spectrum and is best categorized histologically. Characteristic features include steatosis, inflammation, hepatocellular ballooning, and fibrosis<sup>[3]</sup>. NAFLD can be further classified as non-alcoholic fatty liver (NAFL) and non-alcoholic steatohepatitis (NASH)<sup>[3]</sup>. NAFL is a less severe form and is defined as the presence of steatosis with no evidence of hepatocellular injury in the form of ballooning of the hepatocytes<sup>[3]</sup>. NASH, on the other hand, is characterized by the presence of hepatic steatosis and inflammation with hepatocyte injury (ballooning) with or without fibrosis<sup>[3]</sup>. These characteristics of NAFLD can facilitate the risk of further disease progression<sup>[1]</sup>. For example, NAFLD has been linked to the progression and development of hepatocellular carcinoma (HCC), the major histological subtype of liver cancer<sup>[1]</sup>. Similarly, it has been associated with metabolic disorders as up to 75% of individuals with NAFLD have been reported to have type II diabetes<sup>[1]</sup>. Thus, understanding the risk factors for NAFLD is of critical public health importance.

Obesity is a well-characterized risk factor for the development of NAFLD. Although it is well known that obesity can be prevented through healthy dietary habits and physical activity<sup>[4,5]</sup>, interventions in a clinical setting have largely been unsuccessful, especially in the long-term<sup>[6,7]</sup>. Thus, recent research has focused on understanding the pathways driving the pathologic processes associated with obesity-induced NAFLD so that therapeutic targets can be identified. Animal models are

critical to this mission and have greatly enhanced our understanding of NAFLD development. Although multiple animal models of NAFLD exist, high-fat-diet (HFD) administration has been a widely used model<sup>[8]</sup>. However, a limitation of this approach is that HFD administration to mice does not appear to induce significant NAFLD progression (*i.e.*, liver cell death, inflammation, or fibrosis) despite reproducibly inciting obesity, the metabolic syndrome, and hepatic steatosis<sup>[8]</sup>. A potential explanation for this phenomenon is that the duration of HFD feedings is not long enough to produce significant NASH even when diet treatment is administered for six months. Therefore, a longer duration of HFD administration may be necessary to recapitulate the pathology seen in the human condition.

The gut microbiome has recently emerged as a culprit in the development of chronic diseases, such as, obesity<sup>[9,10]</sup>, diabetes<sup>[11,12]</sup>, liver disease<sup>[13,14]</sup>, and cancer<sup>[15]</sup>. In the case of NAFLD, the location of the portal vein allows easy access for bacteria and microbial-derived products to translocate from the gut to the liver<sup>[16]</sup>. In support of this hypothesis, studies conducted in obese humans with NAFLD revealed gut dysbiosis when compared to healthy humans<sup>[17,18]</sup>. Raman *et al*<sup>[17]</sup> reported an enrichment of *Lactobacillus* species and various microbes from the *Firmicutes* phylum in obese humans with NAFLD. Meanwhile, Wong *et al*<sup>[18]</sup>, observed that NASH patients had lower fecal abundance of *Firmicutes*. Although studies examining the link between human gut microbiota and liver diseases have advanced our understanding of this relationship, preclinical models mimicking gut dysbiosis in NAFLD are still lacking<sup>[19]</sup>.

We sought to examine the effects of chronic HFD feeding on NAFLD in mice. C57BL/6 mice were used given their susceptibility to HFD-induced obesity. We utilized a diet consisting of 60% fat, 20% protein, and 20% carbohydrate, which was fed to the mice for a period of 80 wk—a protocol designed to mimic lifetime consumption of a diet high in fat. Our analysis focused largely on liver pathology, fibrosis, inflammation, and endoplasmic reticulum (ER) stress. We also measured metabolic outcomes and characterized fecal microbiota using 16S rRNA sequencing. Our data indicate that chronic HFD consumption does result in significant NAFLD and gut-bacterial dysbiosis. Specifically, we report a significant increase in steatosis, inflammation, cell injury, fibrosis, and ER stress, which was associated with increases in the *Actinobacteria* and *Firmicutes* phylum and decreases in the *Bacteroidetes* and *Tenericutes* phylum.

## MATERIALS AND METHODS

### **Animals and diet**

All procedures involving animals were reviewed and approved by the Institutional Animal Care and Use Committee at the University of South Carolina (animal protocol number, 2044-100482-093011). A total of 53 C57BL/6 male mice were obtained from Jackson Laboratories. Mice (3-5 per cage, wood bedding with nesting material) were kept in a 12:12 h dark/light cycle, in a humidity and temperature control room, and *ad libitum* access to food and water. Animal handling and experiments were performed to minimize pain and discomfort. At 10 wk of age, male mice were randomly assigned to one of two diets for the duration of 80 wk: Low-fat diet (old-LFD, *n* = 15) from Harlan Teklad Rodent Diet, no 8604 (14% Fat, 54% carbohydrate, 32% protein) or High-Fat Diet (Old-HFD, *n* = 18) from Research Diets, D12492 (60% Fat, 20% carbohydrate, 20% protein). An additional group of male mice (10 wk of age) was maintained on the LFD (Young-LFD, *n* = 20) but for a shorter duration (6 wk) to distinguish between age-dependent and age-independent effects of obesity on metabolic, molecular, and histological measures. All three groups of mice were euthanized (overdose of isoflurane) the same day, and fat depots (epididymal, retroperitoneal, and mesentery), liver, and spleen were removed and weighed. The livers were collected and stored at -80 °C or fixed in 4% paraformaldehyde for further analysis.

### **Metabolic measurements and assays**

A day prior to euthanasia, ten mice per each group were fasted for five hours (light cycle). Blood collection was carried out in conscious animals, the tip of the tail was cut with scissors and heparinized capillary tubes (0.12 cm diameter, 7.5 cm length) were used to collect 70 µL of blood from the tail vein for the measurement of glucose and insulin. Blood glucose was assessed using a glucometer (Bayer Counter, New Jersey, United States) and plasma insulin was determined using a mouse ELISA assay from Mercodia (Uppsala, Sweden). Insulin resistance was calculated by HOMA index using the following equation  $IR = (\text{insulin } \mu\text{U/mL}) (\text{glucose mmol/L}) / 22.5$ .

**Staining**

Liver, colon, and adipose tissue were fixed in 4% paraformaldehyde, paraffin-embedded, sectioned, and then stained with hematoxylin eosin (HE). Picro-sirius red stain kit (Cat ab150681, abcam, Cambridge, MA, United States) was used according to the manufacturer's instructions to stain the liver for histological evaluation of fibrosis. For Oil red O staining, frozen liver tissues were cut (10 µm) using a cryostat (Leica Biosystems, Nussloch, Germany) and staining was performed as previously described<sup>[20]</sup>.

**Histopathology**

Histological scoring system for NAFLD was achieved based on HE and picro-sirius red staining in the liver of Young-LFD ( $n = 6$ ), Old-LFD ( $n = 10$ ), and Old-HFD ( $n = 12$ ) mice as previously described<sup>[21]</sup>. A certified pathologist (I.C.) blindly evaluated the histological findings of steatosis (0-3), portal and lobular inflammation (0-3), cell injury (0-2), and fibrosis (0-4) in the liver sections. NAFLD Activity Score (NAS) was calculated by adding the unweighted scores for steatosis, lobular inflammation, cell injury (0-8).

**Western blotting**

Briefly, liver was homogenized in Mueller Buffer containing a protease inhibitor cocktail (Sigma Aldrich, St. Louis, MO, United States). Total protein concentrations were determined by the Bradford method. Equal amounts of crude protein homogenates (20 µg) were fractioned on hand-casted SDS-polyacrylamide gels and electrophoretically transferred to a PVDF membrane using a Royal Genie Blotter (IDEA Scientific, Minneapolis, MN, United States). Membranes were stained with a Ponceau S solution in order to verify equal protein loading and transfer efficiency. Western blots were performed using primary antibodies from Cell Signaling (Danvers, MA, United States) (phosphorylated-IRE1α, IRE1α, XBP1, phosphorylated-EIF2α, EIF2α, phosphorylated-Jnk, Jnk, CHOP, β-actin, phosphorylated-NFκB, NFκB), AbD Serotec Raleigh, NC (F4/80), and Novus Biologicals Littleton, CO (phosphorylated-IRE1α).

**Quantitative real-time PCR**

Gene expression in liver and colon tissue was performed in duplicate after RNA isolation with trizol reagent. The following Taqman gene expression assays from Applied Biosystems were used: Monocyte chemoattractant protein-1 (MCP-1), interleukin 10 (IL-10), interleukin 17-alpha (IL-17α), interleukin 6 (IL-6), forkhead box P3 (Foxp3), or tumor necrosis factor alpha (TNF-α). All primers were normalized to 18s rRNA.

**Microbiome analysis**

Before sacrifice, mice were individually placed in autoclaved cages with no bedding for the collection of three or more fecal pellets per mouse. Fecal pellets were frozen immediately after collection and stored at -80 °C. Isolation and concentration of microbial DNA was achieved using the QIAamp Fast DNA Stool Mini Kit (cat number: 51604, QIAGEN) and a nanophotometer Pearl, respectively. Characterization of the fecal microbiota via 16S rRNA sequencing was performed via the amplification of the 16S rRNA V3 and V4 hypervariable regions. We used 16S V3 314F forward and V4 805R reverse primers, respectively (5'TCGTCGGCAGCGTCAGATGTGTATAAGAGACAGCCTACGGGNGGCWGCAG3' & 5'GTCTCGTGGGCTCGGAGATGTGTATAAGAGACAG GACTACHVGG GTATCTAATCC3') with added Illumina adapter overhang nucleotide sequences<sup>[22]</sup>. The PCR conditions used were 3 min at 95 °C followed by 25 cycles of 30 s at 95 °C, 30 s at 55 °C, 30 s at 72 °C, and a final extension at 72 °C for 5 min. Each reaction mixture (25 µL) contained 50 ng of genomic DNA, 0.5 µL of amplicon PCR forward primer (0.2 µmol/L), 0.5 µL of amplicon PCR reverse primer (0.2 µmol/L) and 12.5 µL of 2× KAPA Hifi Hot Start Ready Mix. Each reaction was cleaned up using Agencourt AMPure XP beads. Attachment of dual indices and Illumina sequencing adapters was performed using 5 µL of amplicon PCR product DNA, 5 µL of Illumina Nextera XT Index Primer 1 (N7xx), 5 µL of Nextera XT Index Primer 2 (S5xx), 25 µL of 2× KAPA HiFi Hot Start Ready Mix, and 10 µL of PCR-grade water. Amplification was carried out under the following conditions: 3 min at 95 °C, followed by 8 cycles of 30 s at 95 °C, 30 s at 55 °C, and 30 s at 72 °C, and a final extension at 72 °C for 5 min. Constructed 16S metagenomic libraries were purified with Agencourt AMPure XP beads and quantified with Quant-iT PicoGreen. Library quality control and average size distribution were determined using an Agilent Technologies 2100 Bioanalyzer. Libraries were normalized and pooled to 40 nmol/L based on quantified values. Pooled samples were denatured and diluted to a final concentration of 6 pmol/L with a 30% PhiX (Illumina) control. Amplicons were



subjected to pyrosequencing using the MiSeq Reagent Kit V3 in the Illumina MiSeq System. The online 16S analysis software from NIH was used to analyze sequencing data collected on the Illumina MiSeq. FASTQ sequences were uploaded to Nephele and the 16S metagenomics application was executed. The groups of related DNA sequences were assigned to operational taxonomic units (OTUs), and output files were analyzed to determine gut microbial composition.

### Statistical analysis

Data from this experiment were analyzed using commercially available statistical software, Prism 5 (GraphPad Software). The statistician, Dr. Bo Cai, from the Department Epidemiology and Biostatistics at the University of South Carolina reviewed the statistical methods of this study. Morphometric measurements, metabolic assays, western blot analysis, and gene expression results were analyzed using a one-way ANOVA followed by Newman-Keuls post hoc test. Kruskal-Wallis test followed by a Dunn's Post-Hoc was used to assess differences in histopathology. A two-tailed Student's t-test and a Mann-Whitney *U* test were used to determine differences in microbiota phylum, family, and genus between Old-LFD and Old-HFD mice. Data that did not pass Barlett's test for equal variances was log-transformed and then re-analyzed. Data are presented as the mean  $\pm$  SE or median with interquartile range. The level of significance was set at  $P < 0.05$ .

## RESULTS

### Morphometric and metabolic analysis of diet-induced NAFLD

To evaluate whether prolonged HFD feeding leads to morphometric and metabolic changes, we determined the mass of three visceral fat depots (epididymal, kidney, and mesentery) and evaluated basal glucose metabolism. As expected, 80 wk of HFD feedings augmented body weight (Figure 1A) in Old-HFD mice when compared to Young-LFD and Old-LFD mice ( $P < 0.05$ ). This increase in body weight was in part due to the significant expansion of epididymal (Figure 1B), kidney (Figure 1C), and mesentery (Figure 1D) fat pads ( $P < 0.05$ ) as well as liver (Figure 1E) and spleen (Figure 1F) tissues. In addition, Old-LFD mice showed a higher body weight and epididymal fat accumulation than Young-LFD mice. Figure 1G, shows a representative histological image of epididymal fat tissue stained with HE; we can observe larger adipocytes surrounded by infiltrated immune cell in Old-HFD mice compared to Old-LFD and Young-LFD mice.

We next addressed whether Old-HFD mice were insulin resistant. As anticipated, Old-HFD mice showed significantly elevated fasting blood glucose (Figure 2A) and insulin (Figure 2B) when compared to Young-LFD and Old-LFD mice ( $P < 0.05$ ). These results were consistent with the HOMA index in which Old-HFD mice exhibited insulin resistance relative to Young-LFD and Old-LFD mice ( $P < 0.05$ ) (Figure 2C). No differences in glucose, insulin, and HOMA index were observed between Old-LFD and Young-LFD mice even though Old-LFD mice displayed an increase in body weight and epididymal fat mass.

### Histopathological assessment of diet-induced NAFLD

In order to evaluate whether prolonged HFD promotes NAFLD, we performed HE, picro-sirius red, and Oil Red O stains in the liver tissue of Young-LFD, Old-LFD, and Old-HFD mice (Figure 3A-C). The analysis of the specimens showed that livers of the Young-LFD mice had minimal focal inflammation, minimal perisinusoidal fibrosis, and no signs of steatosis (NAS score 0-1) (Figure 3D-J). Old-LFD mice displayed mild focal inflammation with focal steatosis, and perisinusoidal fibrosis (NAS score 1-2). In the case of Old-HFD mice, we observed extensive steatosis, portal and lobular inflammation with cell injury (ballooning degeneration of the hepatocytes), and evident fibrosis (NAS score 5-6). We next confirmed fat accumulation in the liver with Oil Red O staining (Figure 3C). Overall, Oil Red O staining provided evidence of macrovesicular accumulation of triglycerides in the hepatocytes of Old-HFD mice when compared to Young-LFD and Old-LFD groups.

### Examination of inflammatory markers in the liver tissue of mice following prolonged HFD feedings

Since inflammation is one of the hallmarks of obesity and NAFLD, we next addressed the question of whether prolonged HFD consumption increases liver inflammation. To assess this, we examined gene expression of MCP-1, IL-6, and TNF- $\alpha$  and the protein concentration of F4/80 and p-NF $\kappa$ B (Figure 4A-E). MCP-1 was significantly elevated in Old-HFD and Old-LFD mice when compared to Young-LFD mice ( $P <$

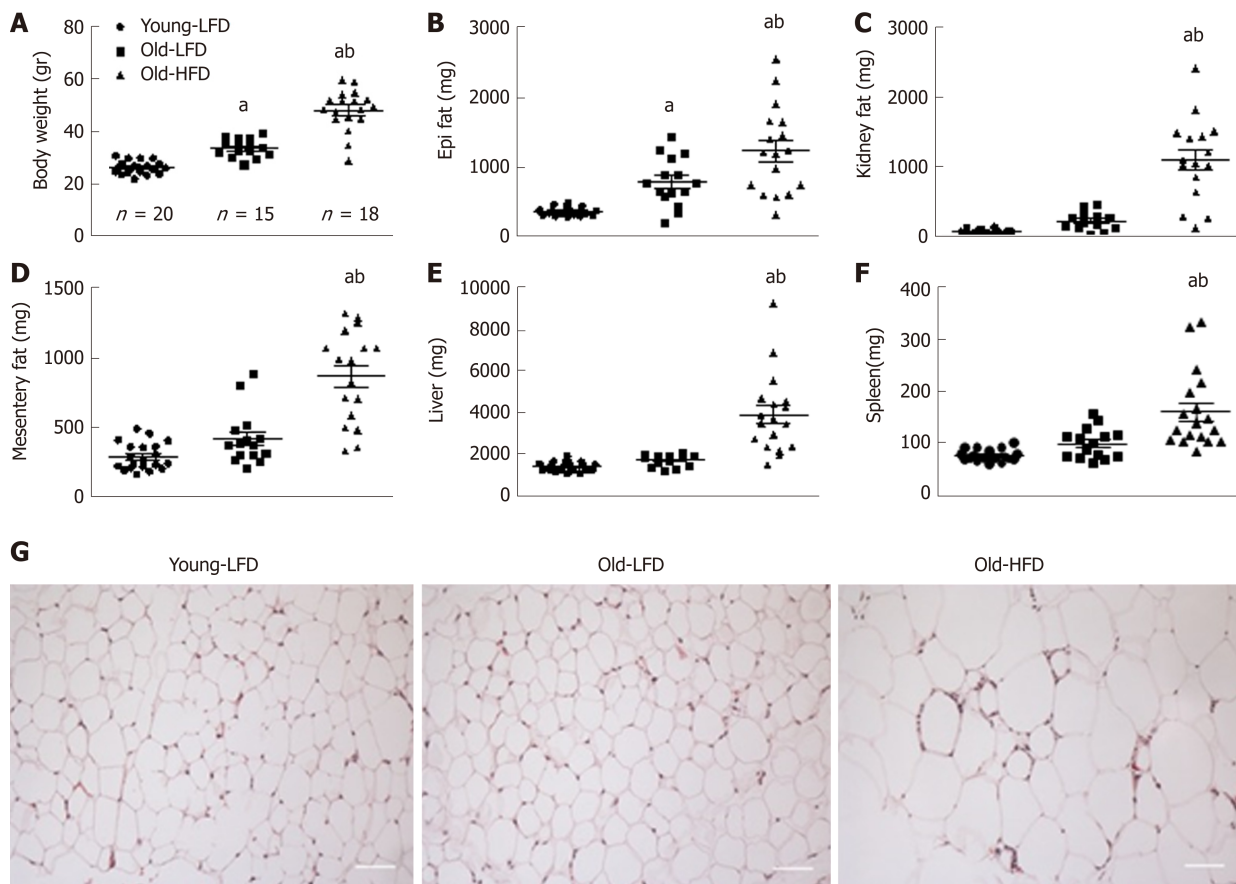


**Figure 1 Morphometric characterization of mice subjected to prolonged high-fat diet-feeding.** A: Average body weight; B: Average mass of epididymal fat pad; C: Kidney fat pad; D: Mesenteric fat pad; E: Liver tissue; F: Spleen tissue. G: Representative hematoxylin and eosin images of epididymal adipose tissue (200 X). Data are expressed as mean  $\pm$  SE.  $n = 15$ -20 mice per group. <sup>a</sup>Significantly different from Young-LFD ( $P < 0.05$ ). <sup>b</sup>Significantly different from Old-LFD ( $P < 0.05$ ). HFD: High-fat diet-feeding; LFD: Low-fat diet.

0.05). Interestingly, F4/80 was significantly decreased with age with a further decrease observed with HFD feeding ( $P < 0.05$ ). No significant changes were observed in the gene expression of IL-6 and TNF- $\alpha$  or the protein expression of p-NF $\kappa$ B.

#### Effects of prolonged HFD feeding on ER stress in the liver

Previous studies have reported that ER stress is involved in the development and progression of steatosis<sup>[23-25]</sup>. Therefore, we next investigated the signaling pathways activated by ER stress, such as, binding immunoglobulin (Bip), inositol-requiring enzyme-1 (IRE1 $\alpha$ ), X-box-binding protein-1 (XBP1s), eukaryotic translation initiation factor 2 $\alpha$  (EIF2 $\alpha$ ), c-Jun-N-terminal kinase (Jnk), and C/EBP-homologous protein (CHOP). There was no change in Bip across the groups (Figure 5A). However, both of the aged groups showed a significant reduction in phosphorylated IRE1 $\alpha$  (Figure 5B) and XBP1s (Figure 5C) when compared to the Young-LFD mice ( $P < 0.05$ ) and there was a further reduction in pIRE1 $\alpha$  with HFD feeding (Old-LFD versus Old-HFD) ( $P < 0.05$ ). For phosphorylated EIF2 $\alpha$  protein expression, there was an elevation in the Old-LFD group compared to Young-LFD and Old-HFD (Figure 5D) ( $P < 0.05$ ). Phosphorylated Jnk was increased in both of the aged groups and there was a further increase with HFD feeding (Figure 5E) ( $P < 0.05$ ). Only the Old-HFD group exhibited an increase in CHOP when compared to Old-LFD and Young-LFD (Figure 5F) ( $P < 0.05$ ).

#### Effects of prolonged HFD feeding on colon inflammation and the gut microbiome profile

To examine whether prolonged HFD feeding produced an inflammatory environment in the colon and/or disrupted the gut microbiome, we analyzed gene expression of inflammatory markers in the colonic tissue and fecal microbial DNA using pyrosequencing. In this study, we did not assess the bacterial composition of the Young-LFD mice, because short-term manipulation of diet is transient<sup>[26]</sup>. A significant increase in IL-6 was observed with age and there was a further increase with HFD feedings (Figure 6C) ( $P < 0.05$ ). Foxp3 was increased in Old-HFD mice when

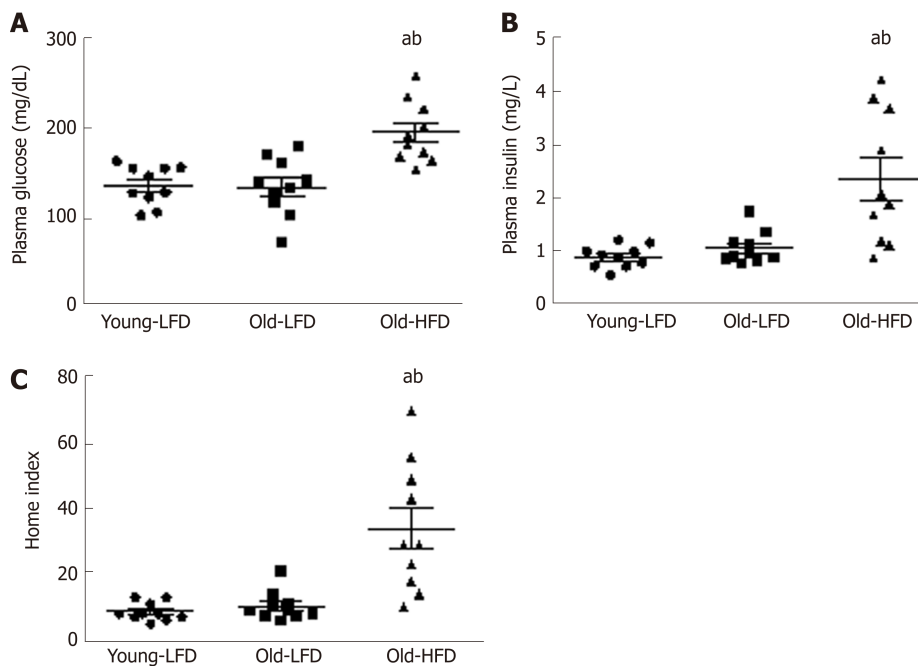


**Figure 2** Metabolic characterization of mice subjected to prolonged high-fat diet-feeding. A: Five hours fasting blood glucose; B: Five hours fasting plasma insulin; C: Homeostasis model of assessment-insulin resistance index. Data are expressed as mean  $\pm$  SE.  $n = 10$  mice per group. <sup>a</sup>Significantly different from Young-LFD ( $P < 0.05$ ). <sup>b</sup>Significantly different from Old-LFD ( $P < 0.05$ ). HOMA-IR: Homeostasis model of assessment-insulin resistance; LFD: Low-fat diet.

compared to Young-LFD and Old-LFD mice ( $P < 0.05$ ) (Figure 6C and E). However, we found no changes in MCP-1, IL-10, or IL-17 $\alpha$  (Figure 6AB, and D) between any of the groups. Representative histological images of the colon tissue in Figure 6F shows similar colonic morphology between groups.

In Figure 7, we observed similar species richness at the taxonomic level (Figure 7A). However, principal coordinate (PC) analysis based on OTU showed distinct gut microbiota composition between Old-LFD and Old-HFD mice (Figure 7B). *Firmicutes* and *Bacteroidetes* were the most predominant phyla in both groups, comprising of 61% and 32% of gut microbiota in Old-LFD mice and 73% and 21% in Old-HFD mice, respectively (Figure 8A and B). Consistently, the ratio of *Firmicutes* to *Bacteroidetes* in Old-HFD mice was altered to favor *Firmicutes* when compared with Old-LFD (Figure 8C,  $P < 0.05$ ). The next two prevalent phylum included *Tenericutes* and *Verrucumicrobia* with 5% and 0.2% of microbiomes in Old-LFD mice and 0.8% and 3.4% in Old-HFD mice, respectively. Prolonged HFD feeding significantly increased the abundance of *Actinobacteria* and *Firmicutes* and decreased the abundance of *Bacteroidetes* and *Tenericutes* when compared to Old-LFD mice ( $P < 0.05$ ). In figure 8D, a positive correlation was observed between body weight and *Firmicutes* abundance ( $P < 0.05$ ), while a negative correlation was observed between body weight and *Bacteroidetes* abundance ( $P < 0.05$ ). At the genus level (Figure 9), we observed a significant increase in the abundance of *Adercreutzia* (Phylum-*Actinobacteria*), *Coprococcus* (Phylum-*Firmicutes*), *Dorea* (Phylum-*Firmicutes*), and *Ruminococcus* (Phylum-*Firmicutes*) in Old-HFD mice when compared to Old-LFD mice ( $P < 0.05$ ). Further, Old-HFD mice showed a decrease in the abundance of *Turicibacter* (Phylum-*Firmicutes*) and *Anaeroplasm* (Phylum-*Tenericutes*) ( $P < 0.05$ ).

## DISCUSSION

In humans, chronic HFD consumption is associated with systemic inflammation, obesity, metabolic dysfunction, NAFLD, and an altered gut microbial profile<sup>[27-29]</sup>. However, animal studies using standard HFD paradigms (16 wk feeding) which mimic obesity, metabolic disorders, and gut microbiota disruption have failed to produce consistent NAFLD pathology<sup>[8,30]</sup> limiting our advancement of mechanistic insights and the development of therapeutic strategies. Therefore, the present study utilized a prolonged HFD feeding (80 wk) to examine NAFLD evolvement. Given that the progression of steatosis to NASH has been linked with changes in inflammation, ER stress<sup>[23]</sup>, and fecal bacterial composition<sup>[17]</sup>, we sought to examine these outcomes in our pre-clinical diet-induced obesity model. In general, we found that prolonged



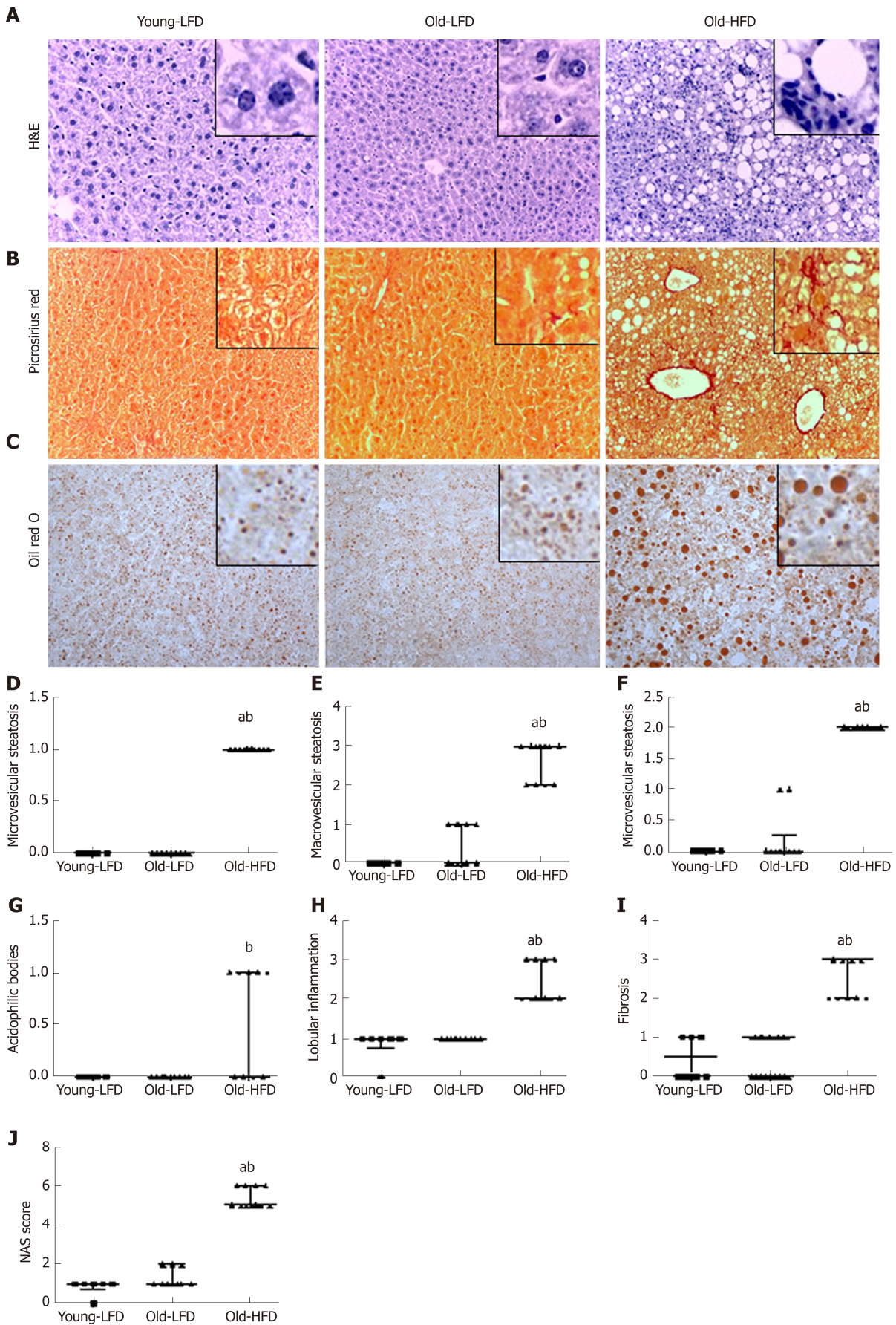


**Figure 3** Histological assessment of the liver tissue in mice subjected to prolonged high-fat diet-feeding. A: Hematoxylin and eosin; B: Picrosirius red; C: Oil red O images of liver tissue (200 X); D: Histological score of microvesicular steatosis; E: Microvesicular steatosis; F: Ballooning degeneration of hepatocytes; G: Acidophilic bodies; H: Lobular inflammation; I: Fibrosis; J: Non-alcoholic steatohepatitis score. Data are expressed as median with interquartile range.  $n = 6-11$  mice per group. <sup>a</sup>Significantly different from Young-LFD ( $P < 0.05$ ), <sup>b</sup>Significantly different from Old-LFD ( $P < 0.05$ ). LFD: Low-fat diet.



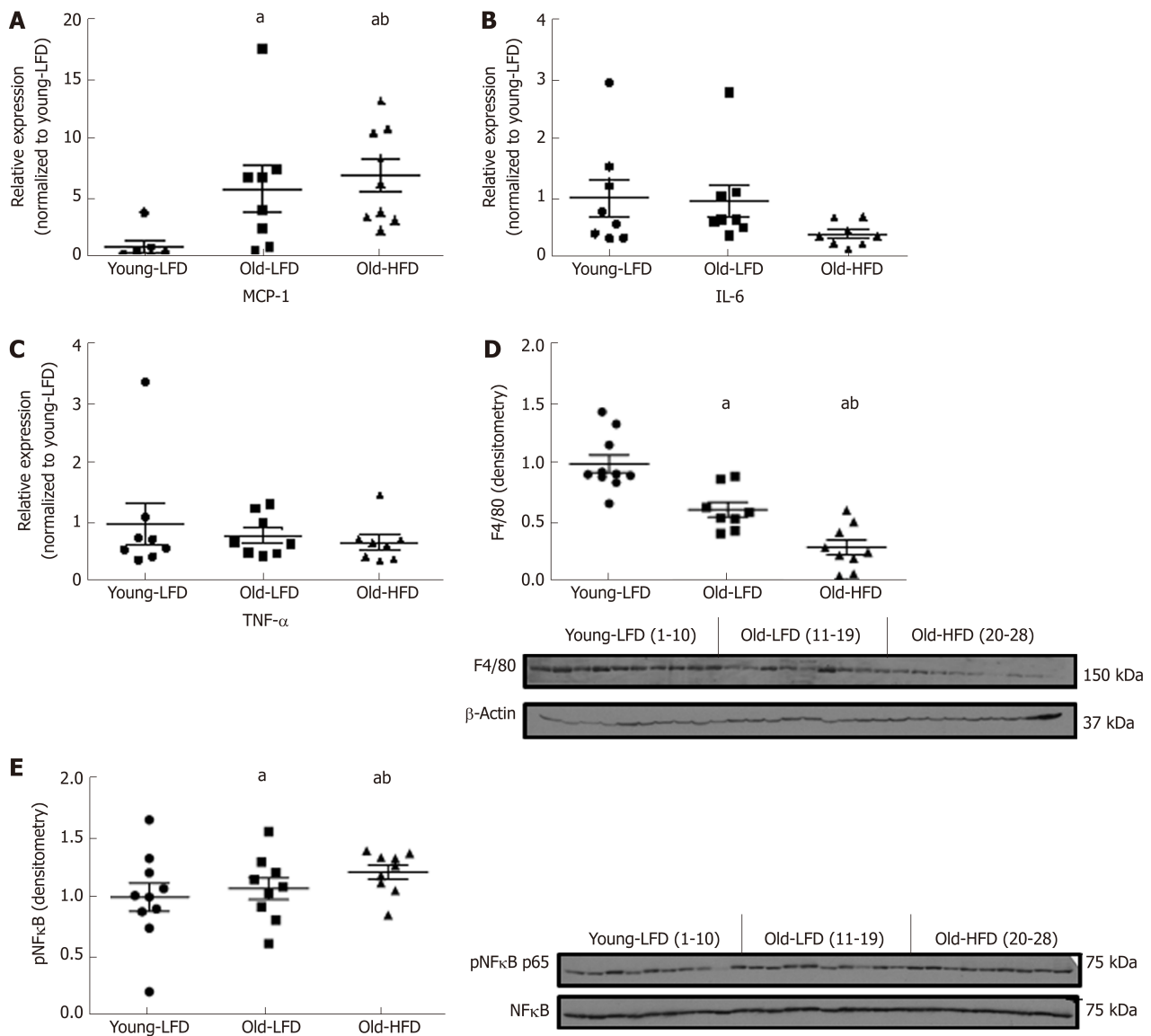


**Figure 4** Inflammatory signaling in the liver tissue of mice subjected to prolonged high-fat diet-feeding. A: Gene expression of monocyte chemoattractant protein-1; B: Gene expression of interleukin; C: Gene expression of tumor necrosis factor alpha; D: Protein concentration of epidermal-growth factor like-like module-containing mucin-like hormone receptor-like 1 also known as F4/80; E: Phosphorylated and total nuclear factor kappa-light-chain-enhancer of activated B cells. Data are expressed as mean  $\pm$  SEM.  $n = 8-10$  mice per group. <sup>a</sup> Significantly different from Young-LFD ( $P < 0.05$ ). <sup>b</sup> Significantly different from Old-LFD ( $P < 0.05$ ). MCP-1: Monocyte chemoattractant protein-1; IL-6: Interleukin 6; TNF $\alpha$ : Tumor necrosis factor alpha; NF $\kappa$ B: Nuclear factor kappa-light-chain-enhancer of activated B cells; LFD: Low-fat diet.

HFD feeding promotes obesity, insulin resistance, ER stress, alterations in gut bacterial composition, and NAFLD in male C57BL/6 mice.

In order to determine if lifetime consumption of a HFD can reliably reproduce NAFLD, we fed mice for a period of 80 wk with a 60% (total kcals) fat diet. NAFLD with 14% kcal from fat and an equal amount of choline as the HFD was used to compare disease outcomes independent of choline deficiency. We controlled for choline given that choline deficient diets have been widely used to induce NAFLD/NASH in rodents<sup>[31,32]</sup>, despite the fact that these diets do not show physiological characteristics involved in the progression of NAFLD/NASH<sup>[33]</sup>. Consistent with our previous studies<sup>[21,34-36]</sup>, we report that HFD consumption increased morphometric parameters (body weight, liver mass, fat pads, and spleen mass) and fasting blood glucose and insulin. Histopathological analysis of the liver indicated that prolonged HFD feeding produced extensive steatosis with portal and lobular inflammation and parenchymal fibrosis in all mice in the Old-HFD group (NAS  $\geq 5$ ). Similar to our findings, others have reported metabolic disturbances and NAFLD pathology using an extended period of HFD feedings<sup>[37,38]</sup>. For example, VanSaun *et al.*<sup>[37]</sup> reported pericellular fibrosis, advanced stage of fibrosis, and NASH after 36, 56, and 80 wk of HFD, respectively. In addition, they observed non-invasive dysplastic tumors in seven of eight mice fed HFD for 36-80 wk. Interestingly, we also

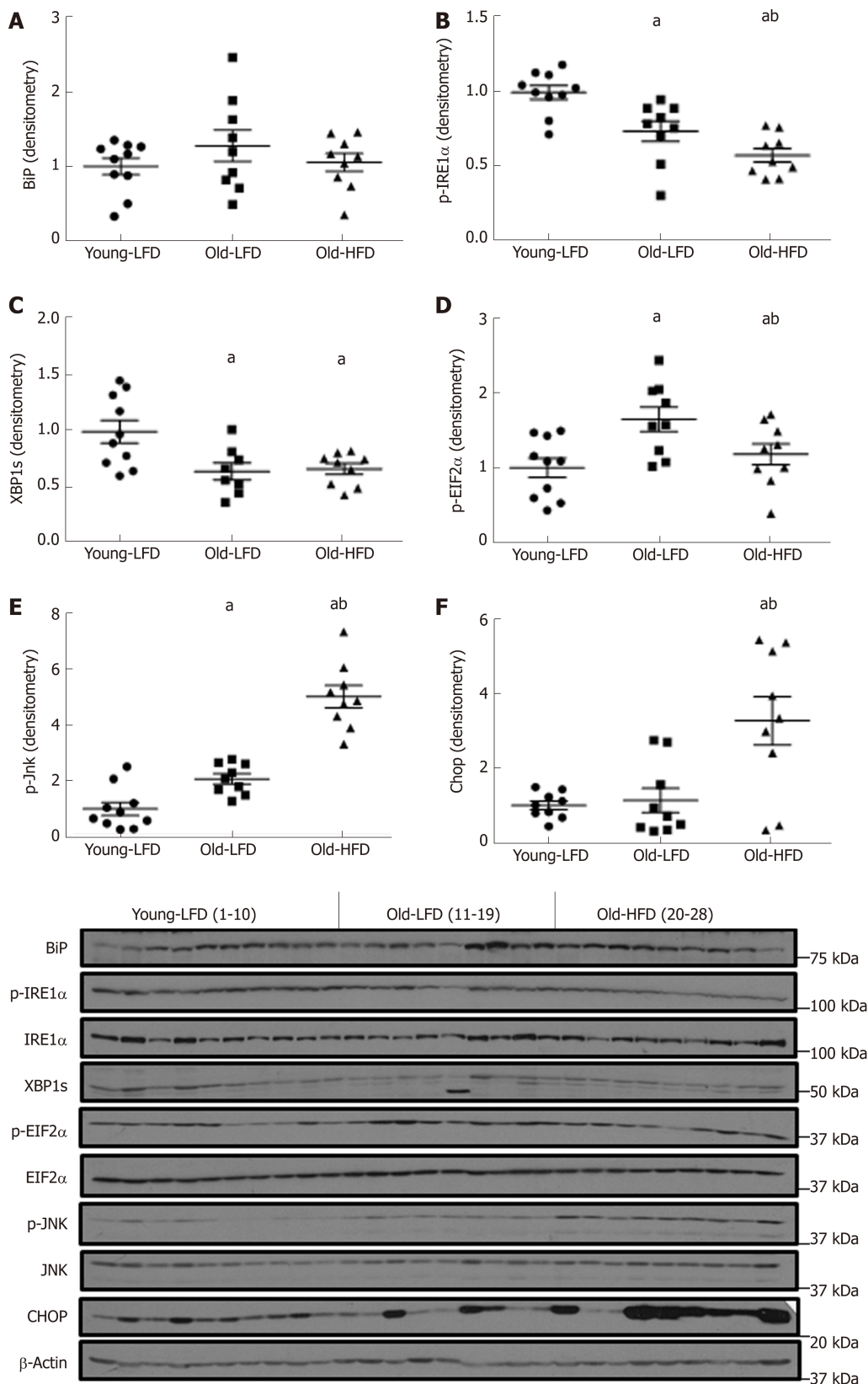


**Figure 5** Endoplasmic reticulum stress signaling in the liver tissue of mice subjected to prolonged high-fat diet-feeding. A: Western blot densitometry analysis of binding immunoglobulin; B: Western blot densitometry analysis of phosphorylated inositol-requiring enzyme-1; C: Western blot densitometry analysis of X-box-binding protein-1; D: Western blot densitometry analysis of phosphorylated eukaryotic translation initiation factor 2 $\alpha$ ; E: Western blot densitometry analysis of phosphorylated c-Jun-N-terminal kinase; F: Western blot densitometry analysis of C/EBP-homologous protein. Data are expressed as mean  $\pm$  SE.  $n = 9-10$  mice per group. <sup>a</sup>Significantly different from Young-LFD ( $P < 0.05$ ). <sup>b</sup>Significantly different from Old-LFD ( $P < 0.05$ ). BiP: Binding immunoglobulin; IRE1 $\alpha$ : Inositol-requiring enzyme-1; XBP1s: X-box-binding protein-1; EIF2 $\alpha$ : Eukaryotic translation initiation factor 2 $\alpha$ ; Jnk: Jun-N-terminal kinas; CHOP: C/EBP-homologous protein; LFD: Low-fat diet.

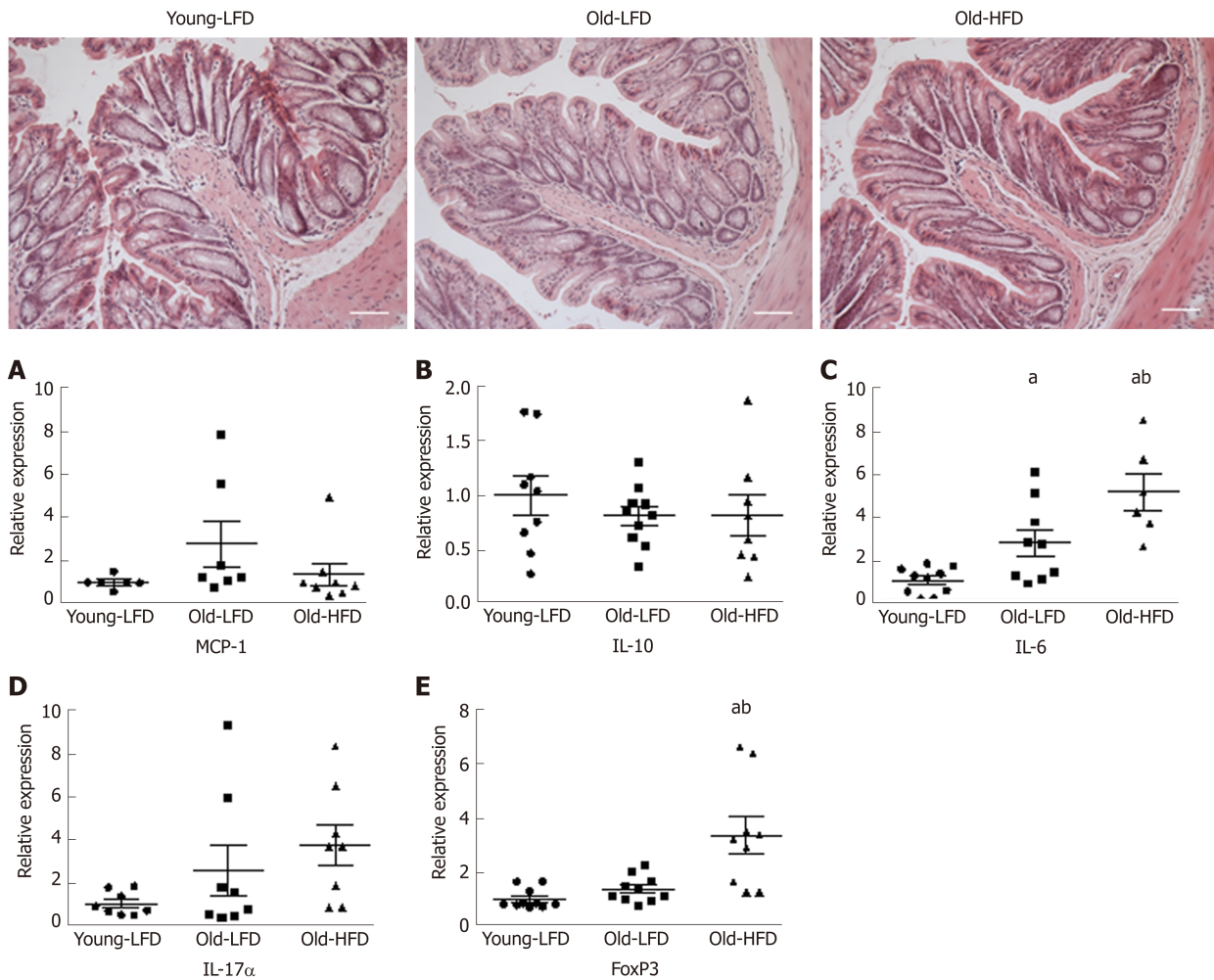


**Figure 6 Inflammatory signaling in the colon tissue of mice subjected to prolonged high-fat diet-feeding.** Representative histology images of colonic tissue (200 X) from Young-low-fat diet (LFD), Old-LFD, and Old-HFD mice. A: Gene expression of Monocyte chemoattractant protein-1 (MCP-1); B: Interleukin 10 (IL-10); C: Interleukin 6 (IL-6); D: Interleukin 17 (IL-17); E: Forkhead box P3 (FoxP3). Data are expressed as mean  $\pm$  SE.  $n = 10$  mice per group. <sup>a</sup> Significantly different from Young-LFD ( $P < 0.05$ ). <sup>b</sup> Significantly different from Old-LFD ( $P < 0.05$ ). HFD: High-fat diet-feeding; LFD: Low-fat diet.

observed non-invasive focal masses in the liver of Old-HFD mice. Young-LFD and Old-LFD mice had an average NAS score of 1, which is not considered diagnostic of steatohepatitis.

Other HFD feeding regimes have been used to mimic the NAFLD condition. However, variability in the degree of NAFLD pathology has been a limitation of these models. For example, the use of the Amylin liver NASH model (AMLN) diet, which is based on a high content of fructose, cholesterol, and trans-fat (partially hydrogenated vegetable oil), has been shown to induce NAFLD stage heterogeneity in mice when the duration of feeding is between 12-30 wk<sup>[39-41]</sup>. However, one study reported that only twenty percent of mice develop liver fibrosis when fed an AMLN diet for a duration of 12 wk<sup>[40]</sup>. Another study reported that key hallmarks of NASH (macrovesicular steatosis and high levels of aspartate aminotransferase) are detected as early as 26 wk after AMLN diet consumption in *Lep<sup>ob/ob</sup>* and C57BL6 mice<sup>[41]</sup>. Nonetheless, not all C57BL/6 mice developed NASH when mice were maintained on an AMLN diet for 30 wk<sup>[39]</sup>. Thus, prolonging the duration of HFD consumption, as in the current study, may be enough to promote a more homogeneous pathology of NAFLD.

The role of pro-inflammatory cytokines in obesity and NAFLD remains unclear. Human studies investigating the action of plasma TNF- $\alpha$  has shown positive or no correlation with insulin resistance in NAFLD and obese patients<sup>[42,43]</sup>. In the case of IL-6, a more clear association has been stipulated between elevated plasma IL-6, insulin resistance, and NAFLD progression<sup>[44,45]</sup>. However, there is no clinical evidence that blocking IL-6 may serve as a treatment for NAFLD and/or metabolic diseases. Additionally, elevated levels of the chemokine MCP-1 also has been observed in NASH and NAFLD patients, which has been correlated with liver fat content<sup>[46-48]</sup>. Our current findings show no differences in the gene expression of TNF $\alpha$  and IL-6 in

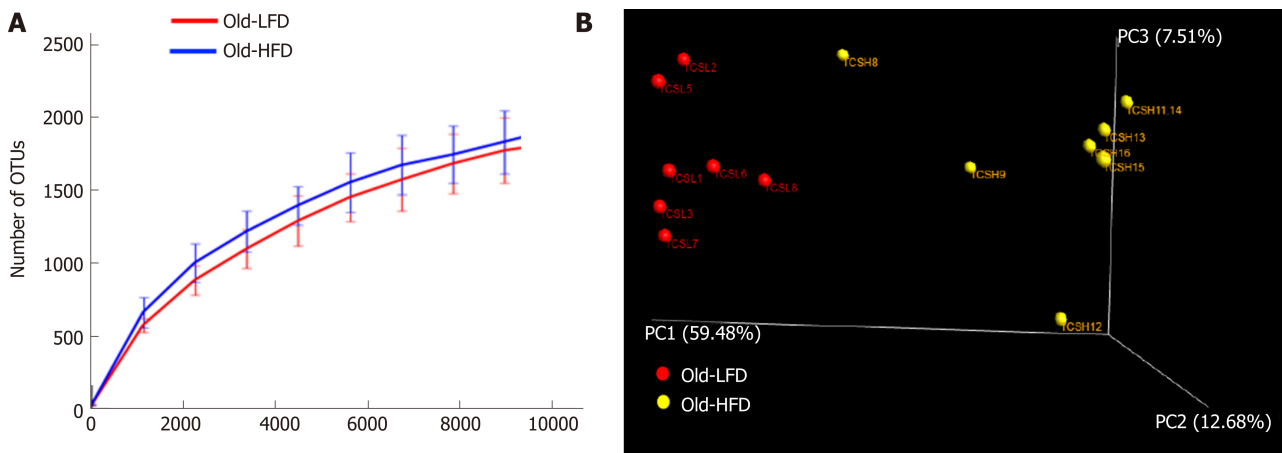


**Figure 7** Gut microbial composition of mice subjected to prolonged high-fat diet-feeding. A: Chao1 and sequence per sample; B: Principal coordinates analysis (PCoA).  $n = 7$  mice per group. Only the feces of Old-high-fat diet-feeding and Old-high-fat diet-feeding mice were analyzed. Data are expressed as mean  $\pm$  SE.  $n = 7$  per group. HFD: High-fat diet-feeding; LFD: Low-fat diet.

mouse liver with NASH pathology. These data coincide with no changes in protein expression of NF $\kappa$ B, a transcription factor involved in inflammatory signaling pathways. Contrary to our hypothesis, a reduction in F4/80 protein expression, a pan macrophage and Kupffer cells marker, was observed in aged mice. This decrease in F4/80 may be a result of aging, as macrophage immune function declines in senescence<sup>[49,50]</sup>. Old-HFD mice showed an even more significant drop in F4/80 than Old-LFD mice, which may be an indication of a depressed immune system related to NAFLD. Interestingly, the gene expression of MCP-1, a major recruiter of macrophages was increased in the liver of both Old-LFD and Old-HFD mice. Given that there was no difference between Old-HFD and Old-LFD groups we believe that this effect is due to aging and not obesity nor NAFLD and likely a compensatory response to the decrease in F4/80 seen in aged mice. It is important to mention that even though we did not find significant changes in the gene expression of TNF- $\alpha$  and IL-6, we did observe significant lobular inflammation in the liver of Old-HFD mice, histologically.

ER stress is associated with obesity, insulin resistance, and NAFLD<sup>[23-25,51]</sup>. It is believed that ER stress can lead to hepatic steatosis by altering lipid metabolism<sup>[52]</sup>. The ER stress response is regulated by three transmembrane proteins: ATF6, IRE1 $\alpha$ , and PKR-like ER kinase (PERK), the molecular chaperone, BiP, and their downstream signaling cascades, including EIF2 $\alpha$  (PERK pathway) and XBP1 activation (IRE1 $\alpha$  pathway), which attempt to bring homeostasis back to the cell under stressful conditions. However, if this is not achieved, chronic ER stress ensues eventually leading to cell death via Jnk and CHOP signaling<sup>[53]</sup> and downregulation of the IRE1 $\alpha$ -XBP1 axis<sup>[54]</sup>. A rapid response to acute ER stress is a significant increase in the production of molecular chaperones, such as BiP<sup>[54]</sup>. We found no differences in the protein expression across groups with respect to BiP; however, we did find a significant decrease in p-IRE1 $\alpha$  and XBP1s in both of the Old groups suggesting that the livers of these mice were experiencing a certain degree of chronic ER stress. Furthermore, the fact that the Old-HFD mice displayed increases in both p-JNK and CHOP protein expression compared to all other groups provides evidence that the chronic consumption of the HFD led to a more advanced stage of chronic ER stress than the Old LFD-treated mice. This is corroborated by the significant increase in p-EIF2 $\alpha$  displayed by the Old-LFD mice and not the Old-HFD mice, as activation of EIF2 $\alpha$ , which inhibits protein translation, typically occurs during the earlier stages of chronic ER stress<sup>[55]</sup>. In fact, Choi *et al*<sup>[56]</sup> demonstrated that inhibition of EIF2 $\alpha$  phosphorylation exacerbates macro-vesicular steatosis, leukocyte infiltration, and fibrosis in mice. Thus, the increased EIF2 $\alpha$  phosphorylation displayed by the Old-LFD mice may be a protective mechanism against the more advanced stages of NAFLD as displayed by the Old-HFD mice.

We also sought to investigate colonic inflammatory cytokines involved in the pathology of colitis due to the co-existence of NAFLD with inflammatory bowel disease (IBD)<sup>[57-61]</sup>. We observed an increase in IL-6 and FoxP3 in the colon tissue of Old-HFD mice, but no changes were observed in MCP-1, IL-10, and IL-17 $\alpha$  between groups. Our findings of an increase in IL-6 is consistent with Jiang *et al*<sup>[62]</sup>, that reported an increase in IL-6 mRNA expression in the intestinal mucosa of NAFLD patients when compared to healthy subjects. Since systemic inflammation including



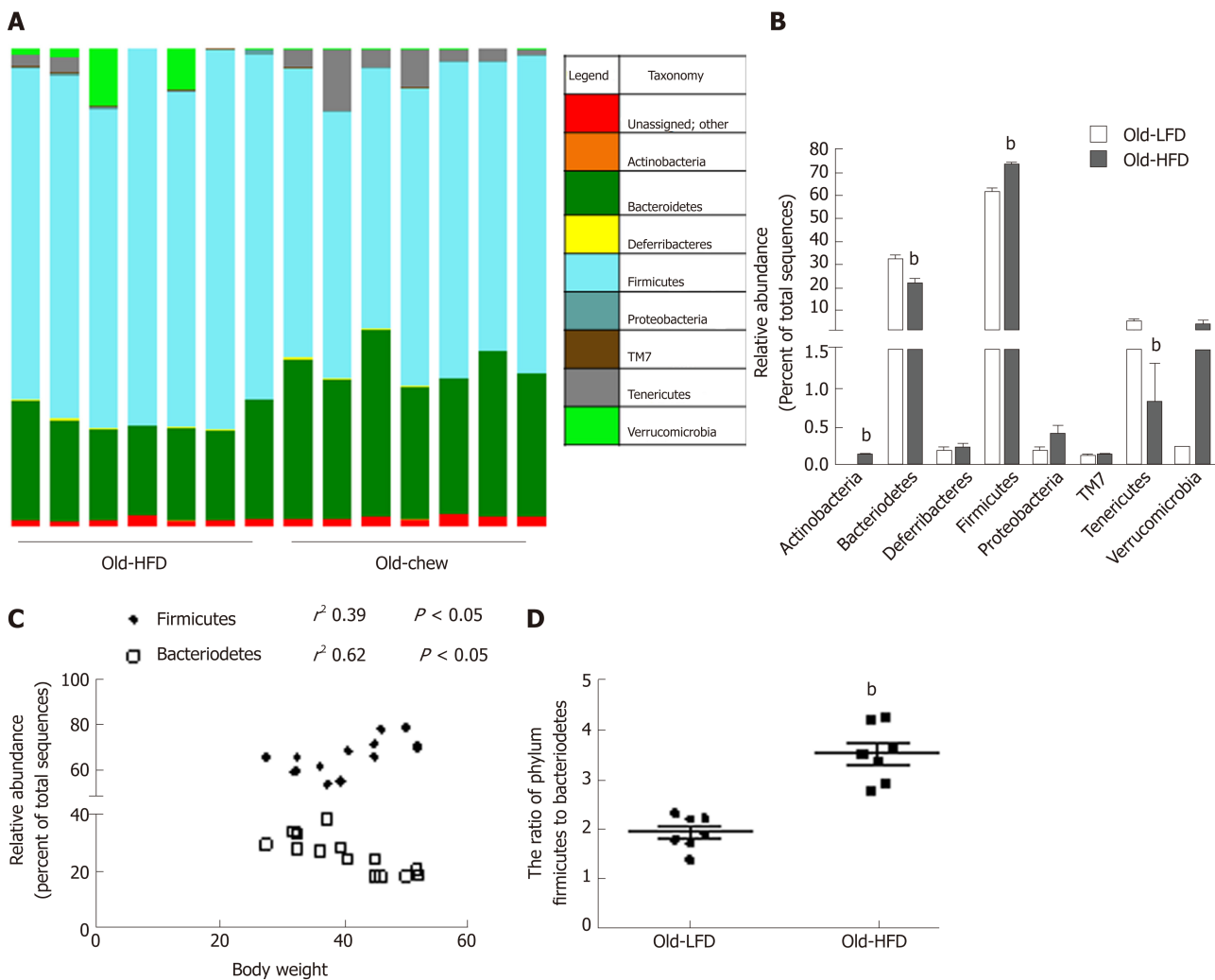


**Figure 8** Relative abundance of gut microbial at the phylum level of mice subjected to prolonged high-fat diet-feeding. A: Bar chart presenting the relative abundance of operational taxonomic units in bacterial phyla; B: Mean relative abundance of phyla; C: Mean relative ratio between *firmicutes* and *bacteroidetes* in Old-low-fat diet (LFD) and Old-high-fat diet-feeding (HFD) mice; D: Correlation between mean relative abundance of *firmicutes* and *bacteroidetes* and mouse body weight. Data are expressed as mean ± SE.  $n = 7$  mice per group. <sup>b</sup>Significantly different from Old-LFD ( $P < 0.05$ ). HFD: High-fat diet-feeding; LFD: Low-fat diet.

IL-6 and TNF- $\alpha$  has been involved in both NAFLD and IBS in humans<sup>[57-61]</sup>, we cannot discard that systemic inflammation and/or gut permeability may play an important role in the development of these disorders. However, we did not measure systemic cytokines nor intestinal permeability in our study. Thus, whether prolonged HFD consumption for 80 wk, as in the current study, exhibits these characteristics remains to be determined. The increase in FoxP3 expression is likely a consequence of the chronic low-grade inflammation in the colon and may explain, in part, the absence of a difference in colon histology.

Studies have reported that the taxonomic composition of gut microbiota in obese individuals indicates a higher proportion of *Firmicutes* and a lower amount of *Bacteroidetes*<sup>[14,19]</sup>. Interestingly, these differences in the ratio of *Firmicutes* and *Bacteroidetes* at the phylum level has been not observed in obese NAFLD patients when compared with age matched healthy control subjects<sup>[17,18,62-68]</sup>. In fact, most of the gut microbiota associated changes in NAFLD and NASH occur at the family and the genus level (Table 1). In general, there is not consistent evidence of a specific family or genus involved in NAFLD/NASH. This could be due, in part, to discrepancies in body mass index, stratification of the disease, sex, diet, and the exclusion or inclusion criteria used across studies. Significant findings in our study include an increase in the abundance of *Firmicutes* and *Actinobacteria* and a decrease in *Bacteroidetes* and *Tenericutes* phlotypes in Old-HFD mice. Consistent with the obesity literature, changes in the *Firmicutes* phylum were positively correlated with body weight while differences in the *Bacteroidetes* phylum were negatively associated with body weight. Since changes in *Firmicutes*, *Actinobacteria* and *Bacteroidetes* have been found when comparing obese NAFLD/NASH and lean healthy children and adolescent patients, we believe that the changes observed in these phyla may be related to the body

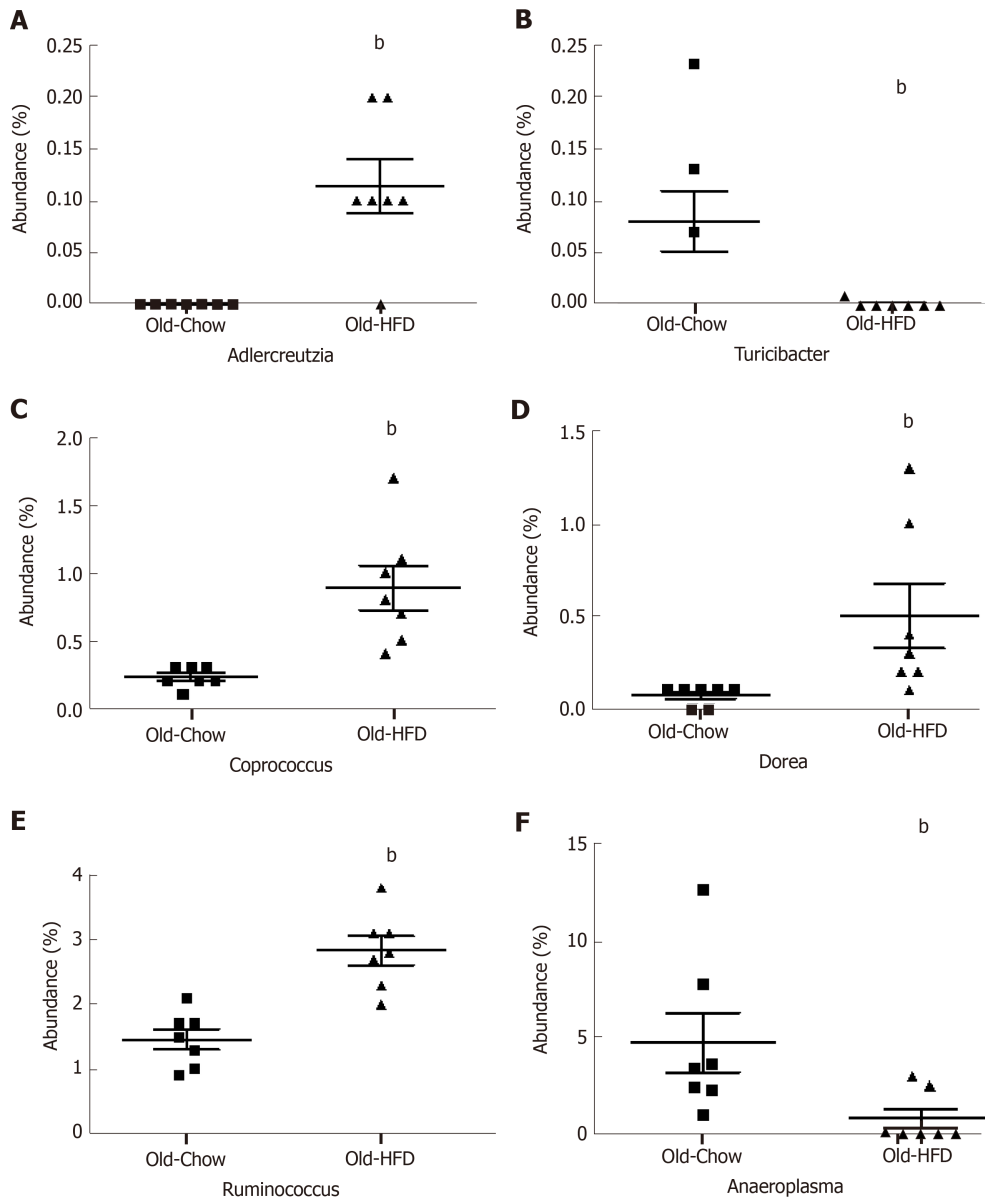


**Figure 9** Relative abundance of gut microbial at the genus level of mice subjected to prolonged high-fat diet-feeding. A: Mean relative abundance of *Adlercreutzia*; B: Mean relative abundance of *Turicibacter*; C: Mean relative abundance of *Coprococcus*; D: Mean relative abundance of *Dorea*; E: Mean relative abundance of *Ruminococcus*; F: Mean relative abundance of *Anaeroplasmia*. Data are expressed as mean  $\pm$  SE.  $n = 7$  mice per group. <sup>b</sup> $P < 0.05$ , vs Old-LFD. HFD: High-fat diet-feeding; LFD: Low-fat diet.

composition and not to the NAFLD pathology. At the genus level, we report an over-representation of *Adlercreutzia*, *Coprococcus*, *Dorea*, and *Ruminococcus* and under-representation of *Turicibacter* and *Anaeroplasmia* abundance in Old-HFD mice. These findings are consistent with some, but not all, of the reported human NAFLD/NASH associated organisms. For example, Raman *et al*<sup>[17]</sup> and Del Chierico *et al*<sup>[65]</sup> reported elevated representation of *Dorea* in NAFLD/NASH children, adolescents, and adult subjects, but Da Silva *et al*<sup>[63]</sup> observed lower abundance of *Dorea* in NAFLD patients. In obese post-menopausal women, *Dorea* genera has been negatively associated with insulin resistance and positively correlated with markers of inflammation<sup>[66]</sup>. Taken together, these studies suggest an association between increased obesity, inflammation, and elevated *Dorea* genera - which may or may not be related to NAFLD. Consistent with our findings, Boursier *et al*<sup>[19]</sup> and Del Chierico *et al*<sup>[65]</sup> observed an increase in the abundance of *Ruminococcus*. Meanwhile, Da Silva *et al*<sup>[63]</sup> observed that NAFLD patients had lower fecal abundance of *Ruminococcus*. Other genera that were altered in the Old-HFD group including *Adlercreutzia*, *Turicibacter*, and *Anaeroplasmia* have not been associated with NAFLD or NASH in human patients. Thus, whether changes in abundance of these microbes is due to diet, obesity, or other factors independent of NAFLD warrants further investigation.

Table 1 Gut microbiota associated changes in non-alcoholic fatty liver disease and Non-alcoholic steatohepatitis subjects

Study	Subjects	Family	Genus
Zhu <i>et al</i> <sup>[14]</sup> , 2012	<sup>3</sup> HC, BMI = 20 kg/m <sup>2</sup>	↑ Prevotellaceae	↑ Prevotella
		↑ Enterobacteriaceae <sup>1</sup>	↑ Escherichia <sup>1</sup>
	<sup>3</sup> Obese, BMI > 30 kg/m <sup>2</sup>	↓ Rikenellaceae	↓ Alistipes
	↓ Actinobacteria	↓ Bifidobacterium	
	<sup>3</sup> NASH, BMI > 30 kg/m <sup>2</sup>	↓ Lachnospiraceae	↓ Blautia
		↓ Ruminococcaceae	↓ Faecalibacterium
Mouzaki <i>et al</i> <sup>[64]</sup> , 2013	HC, BMI = 26 kg/m <sup>2</sup>	↑ Enterobacteriaceae	↑ Clostridium coccoides <sup>2</sup>
	SS, BMI = 29 kg/m <sup>2</sup>	↓ Lachnospiraceae <sup>2</sup>	
Raman <i>et al</i> <sup>[17]</sup> , 2013	HC, BMI < 25 kg/m <sup>2</sup>	↑ Kiloniellaceae	↑ Lactobacillus
		↑ Pasteurellaceae	↑ Robisoniella
	NAFLD, BMI > 30 kg/m <sup>2</sup>	↑ Lactobacillaceae	↑ Roseburia
		↑ Lachnospiraceae	↑ Dorea
		↑ Veillonellaceae	↓ Oscillibacter
		↓ Ruminococcaceae	
		↓ Porphyromonadaceae	
		Clostridiales	↓ Anaerospobacter
Wong <i>et al</i> <sup>[18]</sup> , 2013	HC, BMI = 22 kg/m <sup>2</sup>	↑ Succinivibrionaceae	↑ Parabacteriodes
		↑ Porphyromonadaceae	↑ Allisonella
	NASH, BMI > 30 kg/m <sup>2</sup>	↓ Unclassified	↓ Faecalibacterium
Jiang <i>et al</i> <sup>[62]</sup> , 2015	HC, BMI = 23 kg/m <sup>2</sup>	↑ Peptostreptococcaceae	↑ Anaerobacter
		↓ Ruminococcaceae	↑ Streptococcus
	NAFLD, BMI = 26 kg/m <sup>2</sup>		↑ Lactobacillus
			↑ Escherichia
			↑ Clostridium XI
			↓ Oscillibacter
			↓ Odoribater
			↓ Alistipes
			↓ Flavonifractor
Boursier <i>et al</i> <sup>[19]</sup> , 2016	HC, BMI > 30 kg/m <sup>2</sup>	↑ Bacteroidaceae	↑ Bacteroides
	NASH, BMI > 30 kg/m <sup>2</sup>	↓ Prevotellaceae	↑ Ruminococcus
		↓ Erysipelotrichaceae	↓ Prevotella
Mouzaki <i>et al</i> <sup>[67]</sup> , 2016	HC, BMI = 27 kg/m <sup>2</sup>		↓ Clostridium leptum
	NASH, BMI > 30 kg/m <sup>2</sup>		
Del Chierico <i>et al</i> <sup>[65]</sup> , 2017	<sup>3</sup> HC, BMI = 18 kg/m <sup>2</sup>	↓ Rikenellaceae <sup>4</sup>	↑ Bradyrhizobium <sup>4</sup>
			↑ Anaerococcus <sup>4</sup>
	<sup>3</sup> Obese, BMI = 26 kg/m <sup>2</sup>		↑ Peptoniphilus <sup>4</sup>
	<sup>3</sup> NAFLD, BMI = 26 kg/m <sup>2</sup>		↑ Propionibacterium acnes <sup>4</sup>
	<sup>3</sup> NASH, BMI = 27 kg/m <sup>2</sup>		↑ Dorea <sup>4</sup>
			↑ Ruminococcus <sup>4</sup>
			↓ Oscillospira <sup>4</sup>
			↑ Lactobacillus mucosae <sup>*12</sup>
Nobili <i>et al</i> <sup>[68]</sup> , 2018	<sup>3</sup> HC, BMI = 18 kg/m <sup>2</sup>		
	<sup>3</sup> Obese, BMI = 26 kg/m <sup>2</sup>		
	<sup>3</sup> NAFLD, BMI = 26 kg/m <sup>2</sup>		
	<sup>3</sup> NASH, BMI = 27 kg/m <sup>2</sup>		
Da Silva <i>et al</i> <sup>[63]</sup> , 2018	HC, BMI = 27 kg/m <sup>2</sup>	↓ Bacteroidaceae	↓ Alistipes
		↓ Lachnospiraceae	↓ Anaerostipes
	NAFLD, BMI > 30 kg/m <sup>2</sup>	↓ Lactobacillaceae	↓ Bacteroides
		↓ Porphyromonadaceae	↓ Blautia
		↓ Rikenellaceae	↓ Coprococcus
			↓ Dorea
			↓ Faecalibacterium

↓ Lactobacillus  
 ↓ Parabacteroides  
 ↓ Roseburia  
 ↓ Ruminococcus

<sup>1</sup>Different from Obese;

<sup>2</sup>Different from Steatosis or non-alcoholic fatty liver disease;

<sup>3</sup>Children and adolescent;

<sup>4</sup>Differences between grouping patients and healthy control. BMI: Body mass index; HC: Healthy control; NAFLD: Non-alcoholic fatty liver disease; NASH: Non-alcoholic steatohepatitis; SS: Steatosis.

A limitation in our study is that we were not able to pinpoint a causal relationship between NAFLD and specific microbes. This is in part due to an inability to dissect changes independent of long-term dietary macronutrient manipulation or obesity – both of which directly impact the composition of gut microbiota<sup>[26]</sup>. In addition, it is important to note that our findings did not recapitulate all of the microbial findings that have been reported in the clinical NAFLD/NASH literature. Therefore, additional mechanistic studies are necessary to determine if any of the intestinal bacteria changes that we observed can promote NAFLD pre-clinically. Further, our study was limited to one-time point; all mice were exposed to chronic HFD feeding for the duration of 80 wk. However, it is certainly possible that a shorter duration of HFD feedings (less than 80 wk) may incite NAFLD pathophysiology; although most likely not to the same degree. It also would have been informative to examine changes across time to fully evaluate factors involved in progression of the disease. A third limitation in our study is that we are not able to conclude if the macronutrient composition of the diet is responsible for NAFLD development or rather the excess calories that intrinsically promotes NAFLD. Thus, it may be advantageous to study energy-dense isocaloric diets with high carbohydrate or fat macronutrient content.

In summary, our study examined the effects of prolonged HFD feeding on NAFLD. In particular, we focused on determining the common features of this animal model with NAFLD and human manifestation of the disease. Our prolonged HFD feeding led to the development of obesity, steatosis, non-alcoholic steatohepatitis, insulin resistance, steatosis, liver ER stress, and gut dysbiosis making it a suitable model for the study of NAFLD. Our results suggest that chronic HFD can mimic most, but not all, of the pathophysiological events observed in NAFLD.

## ARTICLE HIGHLIGHTS

### Research background

Animal models that can exhibit characteristics seen in non-alcoholic fatty liver disease (NAFLD) have the potential to drive the discovery of new drugs to treat this disease.

### Research motivation

Most animal models used to investigate NAFLD misrepresent typical characteristics seen in human patients with NAFLD. Therefore, any successful treatments documented in these animal models may not be clinically translatable.

### Research objectives

To evaluate if mice consuming a high calorie diet for a prolonged time can mimic clinical characteristics of NAFLD.

### Research methods

Male mice (10 wk old) were assigned to the following groups: Young- low-fat diet (LFD) ( $n = 20$ ; low calorie diet for), Old-LFD ( $n = 15$ ; low calorie diet), and Old-HFD ( $n = 18$ ; high calorie diet). Mice in the LFD consumed a diet rich in carbohydrates, meanwhile the HFD was abundant in fat content. Liver, colon, adipose tissue, and feces were collected at 16 wk of age in Young-LFD mice and at 90 wk of age in Old-LFD and Old-HFD to evaluate microscopic features, glucose metabolism, inflammation, endoplasmic reticulum (ER) stress, and microbiome profile seen in NAFLD.

### Research results

Old-HFD mice showed increased body weight, blood glucose, plasma insulin, HOMA index, steatosis, hepatocellular ballooning, inflammation, fibrosis, NAFLD activity score, ER stress markers (CHOP and p-Jnk), and abundance of *Firmicutes*, *Adlercreutzia*, *Turicibacter*, *Coproccoccus*, *Dorea*, and *Ruminococcus*.

### Research conclusions

Mice fed a high calorie diet for 80-wk (Old-HFD) mimicked microscopic characteristic and



microbial events that have been previously observed in NAFLD patients.

### Research perspectives

It is important to critically select animal models to study any disease including NAFLD. Future research dedicated to investigation of new treatments for NAFLD should consider prolonged-HFD feedings as their animal model.

## REFERENCES

- 1 **Younossi ZM**, Otgonsuren M, Henry L, Venkatesan C, Mishra A, Erario M, Hunt S. Association of nonalcoholic fatty liver disease (NAFLD) with hepatocellular carcinoma (HCC) in the United States from 2004 to 2009. *Hepatology* 2015; **62**: 1723-1730 [PMID: 26274335 DOI: 10.1002/hep.28123]
- 2 **Federico A**, Zulli C, de Sio I, Del Prete A, Dallio M, Masarone M, Loguercio C. Focus on emerging drugs for the treatment of patients with non-alcoholic fatty liver disease. *World J Gastroenterol* 2014; **20**: 16841-16857 [PMID: 25492998 DOI: 10.3748/wjg.v20.i45.16841]
- 3 **Chalasani N**, Younossi Z, Lavine JE, Diehl AM, Brunt EM, Cusi K, Charlton M, Sanyal AJ; American Gastroenterological Association; American Association for the Study of Liver Diseases; American College of Gastroenterology. The diagnosis and management of non-alcoholic fatty liver disease: practice guideline by the American Gastroenterological Association, American Association for the Study of Liver Diseases, and American College of Gastroenterology. *Gastroenterology* 2012; **142**: 1592-1609 [PMID: 22656328 DOI: 10.1053/j.gastro.2012.04.001]
- 4 **Fox KR**, Hillsdon M. Physical activity and obesity. *Obes Rev* 2007; **8** Suppl 1: 115-121 [PMID: 17316313 DOI: 10.1111/j.1467-789X.2007.00329.x]
- 5 **Wareham NJ**, van Sluijs EM, Ekelund U. Physical activity and obesity prevention: a review of the current evidence. *Proc Nutr Soc* 2005; **64**: 229-247 [PMID: 15960868]
- 6 **Roberts DL**, Dive C, Renehan AG. Biological mechanisms linking obesity and cancer risk: new perspectives. *Annu Rev Med* 2010; **61**: 301-316 [PMID: 19824817 DOI: 10.1146/annurev.med.080708.082713]
- 7 **Lemmens VE**, Oenema A, Klepp KI, Henriksen HB, Brug J. A systematic review of the evidence regarding efficacy of obesity prevention interventions among adults. *Obes Rev* 2008; **9**: 446-455 [PMID: 18298429 DOI: 10.1111/j.1467-789X.2008.00468.x]
- 8 **Asai A**, Chou PM, Bu HF, Wang X, Rao MS, Jiang A, DiDonato CJ, Tan XD. Dissociation of hepatic insulin resistance from susceptibility of nonalcoholic fatty liver disease induced by a high-fat and high-carbohydrate diet in mice. *Am J Physiol Gastrointest Liver Physiol* 2014; **306**: G496-G504 [PMID: 24436353 DOI: 10.1152/ajpgi.00291.2013]
- 9 **Turnbaugh PJ**, Hamady M, Yatsunenko T, Cantarel BL, Duncan A, Ley RE, Sogin ML, Jones WJ, Roe BA, Affourtit JP, Egholm M, Henriksen B, Heath AC, Knight R, Gordon JI. A core gut microbiome in obese and lean twins. *Nature* 2009; **457**: 480-484 [PMID: 19043404 DOI: 10.1038/nature07540]
- 10 **Murphy EF**, Cotter PD, Hogan A, O'Sullivan O, Joyce A, Fouchy F, Clarke SF, Marques TM, O'Toole PW, Stanton C, Quigley EM, Daly C, Ross PR, O'Doherty RM, Shanahan F. Divergent metabolic outcomes arising from targeted manipulation of the gut microbiota in diet-induced obesity. *Gut* 2013; **62**: 220-226 [PMID: 22345653 DOI: 10.1136/gutjnl-2011-300705]
- 11 **Larsen N**, Vogensen FK, van den Berg FW, Nielsen DS, Andreasen AS, Pedersen BK, Al-Soud WA, Sørensen SJ, Hansen LH, Jakobsen M. Gut microbiota in human adults with type 2 diabetes differs from non-diabetic adults. *PLoS One* 2010; **5**: e9085 [PMID: 20140211 DOI: 10.1371/journal.pone.0009085]
- 12 **Qin J**, Li Y, Cai Z, Li S, Zhu J, Zhang F, Liang S, Zhang W, Guan Y, Shen D, Peng Y, Zhang D, Jie Z, Wu W, Qin Y, Xue W, Li J, Han L, Lu D, Wu P, Dai Y, Sun X, Li Z, Tang A, Zhong S, Li X, Chen W, Xu R, Wang M, Feng Q, Gong M, Yu J, Zhang Y, Zhang M, Hansen T, Sanchez G, Raes J, Falony G, Okuda S, Almeida M, LeChatelier E, Renault P, Pons N, Batto JM, Zhang Z, Chen H, Yang R, Zheng W, Li S, Yang H, Wang J, Ehrlich SD, Nielsen R, Pedersen O, Kristiansen K, Wang J. A metagenome-wide association study of gut microbiota in type 2 diabetes. *Nature* 2012; **490**: 55-60 [PMID: 23023125 DOI: 10.1038/nature11450]
- 13 **Boursier J**, Diehl AM. Implication of gut microbiota in nonalcoholic fatty liver disease. *PLoS Pathog* 2015; **11**: e1004559 [PMID: 25625278 DOI: 10.1371/journal.ppat.1004559]
- 14 **Zhu L**, Baker SS, Gill C, Liu W, Alkhouli R, Baker RD, Gill SR. Characterization of gut microbiomes in nonalcoholic steatohepatitis (NASH) patients: a connection between endogenous alcohol and NASH. *Hepatology* 2013; **57**: 601-609 [PMID: 23055155 DOI: 10.1002/hep.26093]
- 15 **Yu LX**, Schwabe RF. The gut microbiome and liver cancer: mechanisms and clinical translation. *Nat Rev Gastroenterol Hepatol* 2017; **14**: 527-539 [PMID: 28676707 DOI: 10.1038/nrgastro.2017.72]
- 16 **Tilg H**, Cani PD, Mayer EA. Gut microbiome and liver diseases. *Gut* 2016; **65**: 2035-2044 [PMID: 27802157 DOI: 10.1136/gutjnl-2016-312729]
- 17 **Raman M**, Ahmed I, Gillevet PM, Probert CS, Ratcliffe NM, Smith S, Greenwood R, Sikaroodi M, Lam V, Crotty P, Bailey J, Myers RP, Rioux KP. Fecal microbiome and volatile organic compound metabolome in obese humans with nonalcoholic fatty liver disease. *Clin Gastroenterol Hepatol* 2013; **11**: 868-875.e1-3 [PMID: 23454028 DOI: 10.1016/j.cgh.2013.02.015]
- 18 **Wong VW**, Tse CH, Lam TT, Wong GL, Chim AM, Chu WC, Yeung DK, Law PT, Kwan HS, Yu J, Sung JJ, Chan HL. Molecular characterization of the fecal microbiota in patients with nonalcoholic steatohepatitis--a longitudinal study. *PLoS One* 2013; **8**: e62885 [PMID: 23638162 DOI: 10.1371/journal.pone.0062885]
- 19 **Boursier J**, Mueller O, Barret M, Machado M, Fizanne L, Araujo-Perez F, Guy CD, Seed PC, Rawls JF, David LA, Hunault G, Oberti F, Calès P, Diehl AM. The severity of nonalcoholic fatty liver disease is associated with gut dysbiosis and shift in the metabolic function of the gut microbiota. *Hepatology* 2016; **63**: 764-775 [PMID: 26600078 DOI: 10.1002/hep.28356]
- 20 **Koopman R**, Schaart G, Hesselink MK. Optimisation of oil red O staining permits combination with immunofluorescence and automated quantification of lipids. *Histochem Cell Biol* 2001; **116**: 63-68 [PMID: 11479724]
- 21 **Velázquez KT**, Enos RT, Carson MS, Cranford TL, Bader JE, Chatzistamou I, Singh UP, Nagarkatti PS, Nagarkatti M, Davis JM, Carson JA, Murphy EA. Weight loss following diet-induced obesity does not

- alter colon tumorigenesis in the AOM mouse model. *Am J Physiol Gastrointest Liver Physiol* 2016; **311**: G699-G712 [PMID: 27609769 DOI: 10.1152/ajpgi.00207.2016]
- 22 **Klindworth A**, Pruesse E, Schweer T, Peplies J, Quast C, Horn M, Glöckner FO. Evaluation of general 16S ribosomal RNA gene PCR primers for classical and next-generation sequencing-based diversity studies. *Nucleic Acids Res* 2013; **41**: e1 [PMID: 22933715 DOI: 10.1093/nar/gks808]
- 23 **Zhang XQ**, Xu CF, Yu CH, Chen WX, Li YM. Role of endoplasmic reticulum stress in the pathogenesis of nonalcoholic fatty liver disease. *World J Gastroenterol* 2014; **20**: 1768-1776 [PMID: 24587654 DOI: 10.3748/wjg.v20.i7.1768]
- 24 **Chambers JE**, Marciniak SJ. Cellular mechanisms of endoplasmic reticulum stress signaling in health and disease. 2. Protein misfolding and ER stress. *Am J Physiol Cell Physiol* 2014; **307**: C657-C670 [PMID: 24944205 DOI: 10.1152/ajpcell.00183.2014]
- 25 **Pagliassotti MJ**. Endoplasmic reticulum stress in nonalcoholic fatty liver disease. *Annu Rev Nutr* 2012; **32**: 17-33 [PMID: 22809102 DOI: 10.1146/annurev-nutr-071811-150644]
- 26 **Wu GD**, Chen J, Hoffmann C, Bittinger K, Chen YY, Keilbaugh SA, Bewtra M, Knights D, Walters WA, Knight R, Sinha R, Gilroy E, Gupta K, Baldassano R, Nessel L, Li H, Bushman FD, Lewis JD. Linking long-term dietary patterns with gut microbial enterotypes. *Science* 2011; **334**: 105-108 [PMID: 21885731 DOI: 10.1126/science.1208344]
- 27 **Martinez KB**, Leone V, Chang EB. Western diets, gut dysbiosis, and metabolic diseases: Are they linked? *Gut Microbes* 2017; **8**: 130-142 [PMID: 28059614 DOI: 10.1080/19490976.2016.1270811]
- 28 **Manzel A**, Muller DN, Hafler DA, Erdman SE, Linker RA, Kleinewietfeld M. Role of "Western diet" in inflammatory autoimmune diseases. *Curr Allergy Asthma Rep* 2014; **14**: 404 [PMID: 24338487 DOI: 10.1007/s11882-013-0404-6]
- 29 **Minihane AM**, Vinoy S, Russell WR, Baka A, Roche HM, Tuohy KM, Teeling JL, Blaak EE, Fenech M, Vauzour D, McArdle HJ, Kremer BH, Sterkman L, Vafeiadou K, Benedetti MM, Williams CM, Calder PC. Low-grade inflammation, diet composition and health: current research evidence and its translation. *Br J Nutr* 2015; **114**: 999-1012 [PMID: 26228057 DOI: 10.1017/S0007114515002093]
- 30 **Le Roy T**, Llopis M, Lepage P, Bruneau A, Rabot S, Bevilacqua C, Martin P, Philippe C, Walker F, Bado A, Perlemuter G, Cassard-Doulcier AM, Gérard P. Intestinal microbiota determines development of non-alcoholic fatty liver disease in mice. *Gut* 2013; **62**: 1787-1794 [PMID: 23197411 DOI: 10.1136/gutjnl-2012-303816]
- 31 **Nakae D**, Mizumoto Y, Andoh N, Tamura K, Horiguchi K, Endoh T, Kobayashi E, Tsujiuchi T, Denda A, Lombardi B. Comparative changes in the liver of female Fischer-344 rats after short-term feeding of a semipurified or a semisynthetic L-amino acid-defined choline-deficient diet. *Toxicol Pathol* 1995; **23**: 583-590 [PMID: 8578101 DOI: 10.1177/019262339502300504]
- 32 **Itagaki H**, Shimizu K, Morikawa S, Ogawa K, Ezaki T. Morphological and functional characterization of non-alcoholic fatty liver disease induced by a methionine-choline-deficient diet in C57BL/6 mice. *Int J Clin Exp Pathol* 2013; **6**: 2683-2696 [PMID: 24294355]
- 33 **Machado MV**, Michelotti GA, Xie G, Almeida Pereira T, Boursier J, Bohnic B, Guy CD, Diehl AM. Mouse models of diet-induced nonalcoholic steatohepatitis reproduce the heterogeneity of the human disease. *PLoS One* 2015; **10**: e0127991 [PMID: 26017539 DOI: 10.1371/journal.pone.0127991]
- 34 **Cranford TL**, Velázquez KT, Enos RT, Sougiannis AT, Bader JE, Carson MS, Bellone RR, Chatzistamou I, Nagarkatti M, Murphy EA. Effects of high fat diet-induced obesity on mammary tumorigenesis in the PyMT/MMTV murine model. *Cancer Biol Ther* 2019; **20**: 487-496 [PMID: 30388923 DOI: 10.1080/15384047.2018.1537574]
- 35 **Velázquez KT**, Enos RT, Carson MS, Cranford TL, Bader JE, Sougiannis AT, Pritchett C, Fan D, Carson JA, Murphy EA. miR155 deficiency aggravates high-fat diet-induced adipose tissue fibrosis in male mice. *Physiol Rep* 2017; **5** [PMID: 28947593 DOI: 10.14814/phy2.13412]
- 36 **Enos RT**, Davis JM, Velázquez KT, McClellan JL, Day SD, Carnevale KA, Murphy EA. Influence of dietary saturated fat content on adiposity, macrophage behavior, inflammation, and metabolism: composition matters. *J Lipid Res* 2013; **54**: 152-163 [PMID: 23103474 DOI: 10.1194/jlr.M030700]
- 37 **VanSaun MN**, Lee IK, Washington MK, Matrisian L, Gorden DL. High fat diet induced hepatic steatosis establishes a permissive microenvironment for colorectal metastases and promotes primary dysplasia in a murine model. *Am J Pathol* 2009; **175**: 355-364 [PMID: 19541928 DOI: 10.2353/ajpath.2009.080703]
- 38 **Hill-Baskin AE**, Markiewski MM, Buchner DA, Shao H, DeSantis D, Hsiao G, Subramaniam S, Berger NA, Croniger C, Lambris JD, Nadeau JH. Diet-induced hepatocellular carcinoma in genetically predisposed mice. *Hum Mol Genet* 2009; **18**: 2975-2988 [PMID: 19454484 DOI: 10.1093/hmg/ddp236]
- 39 **Clapper JR**, Hendricks MD, Gu G, Wittmer C, Dolman CS, Herich J, Athanacio J, Villescaz C, Ghosh SS, Heilig JS, Lowe C, Roth JD. Diet-induced mouse model of fatty liver disease and nonalcoholic steatohepatitis reflecting clinical disease progression and methods of assessment. *Am J Physiol Gastrointest Liver Physiol* 2013; **305**: G483-G495 [PMID: 23886860 DOI: 10.1152/ajpgi.00079.2013]
- 40 **Trevaskis JL**, Griffin PS, Wittmer C, Neuschwander-Tetri BA, Brunt EM, Dolman CS, Erickson MR, Napora J, Parkes DG, Roth JD. Glucagon-like peptide-1 receptor agonism improves metabolic, biochemical, and histopathological indices of nonalcoholic steatohepatitis in mice. *Am J Physiol Gastrointest Liver Physiol* 2012; **302**: G762-G772 [PMID: 22268099 DOI: 10.1152/ajpgi.00476.2011]
- 41 **Kristiansen MN**, Veidal SS, Rigbolt KT, Tølbøl KS, Roth JD, Jelsing J, Vrang N, Feigh M. Obese diet-induced mouse models of nonalcoholic steatohepatitis-tracking disease by liver biopsy. *World J Hepatol* 2016; **8**: 673-684 [PMID: 27326314 DOI: 10.4254/wjh.v8.i16.673]
- 42 **Lesmana CR**, Hasan I, Budihusodo U, Gani RA, Krisnuhoni E, Akbar N, Lesmana LA. Diagnostic value of a group of biochemical markers of liver fibrosis in patients with non-alcoholic steatohepatitis. *J Dig Dis* 2009; **10**: 201-206 [PMID: 19659788 DOI: 10.1111/j.1751-2980.2009.00386.x]
- 43 **Li W**, Zheng L, Sheng C, Cheng X, Qing L, Qu S. Systematic review on the treatment of pentoxifylline in patients with non-alcoholic fatty liver disease. *Lipids Health Dis* 2011; **10**: 49 [PMID: 21477300 DOI: 10.1186/1476-511X-10-49]
- 44 **Kugelmas M**, Hill DB, Vivian B, Marsano L, McClain CJ. Cytokines and NASH: a pilot study of the effects of lifestyle modification and vitamin E. *Hepatology* 2003; **38**: 413-419 [PMID: 12883485 DOI: 10.1053/jhep.2003.50316]
- 45 **Wieckowska A**, Papouchado BG, Li Z, Lopez R, Zein NN, Feldstein AE. Increased hepatic and circulating interleukin-6 levels in human nonalcoholic steatohepatitis. *Am J Gastroenterol* 2008; **103**: 1372-1379 [PMID: 18510618 DOI: 10.1111/j.1572-0241.2007.01774.x]
- 46 **Haukeland JW**, Damås JK, Konopski Z, Løberg EM, Haaland T, Goverud I, Torjesen PA, Birkeland K, Bjørø K, Aukrust P. Systemic inflammation in nonalcoholic fatty liver disease is characterized by elevated

- levels of CCL2. *J Hepatol* 2006; **44**: 1167-1174 [PMID: [16618517](#) DOI: [10.1016/j.jhep.2006.02.011](#)]
- 47 **Westerbacka J**, Kolak M, Kiviluoto T, Arkkila P, Sirén J, Hamsten A, Fisher RM, Yki-Järvinen H. Genes involved in fatty acid partitioning and binding, lipolysis, monocyte/macrophage recruitment, and inflammation are overexpressed in the human fatty liver of insulin-resistant subjects. *Diabetes* 2007; **56**: 2759-2765 [PMID: [17704301](#) DOI: [10.2337/db07-0156](#)]
- 48 **Greco D**, Kotronen A, Westerbacka J, Puig O, Arkkila P, Kiviluoto T, Laitinen S, Kolak M, Fisher RM, Hamsten A, Auvinen P, Yki-Järvinen H. Gene expression in human NAFLD. *Am J Physiol Gastrointest Liver Physiol* 2008; **294**: G1281-G1287 [PMID: [18388185](#) DOI: [10.1152/ajpgi.00074.2008](#)]
- 49 **Linehan E**, Fitzgerald DC. Ageing and the immune system: focus on macrophages. *Eur J Microbiol Immunol (Bp)* 2015; **5**: 14-24 [PMID: [25883791](#) DOI: [10.1556/EUJMI-D-14-00035](#)]
- 50 **Stahl EC**, Haschak MJ, Popovic B, Brown BN. Macrophages in the Aging Liver and Age-Related Liver Disease. *Front Immunol* 2018; **9**: 2795 [PMID: [30555477](#) DOI: [10.3389/fimmu.2018.02795](#)]
- 51 **Kim OK**, Jun W, Lee J. Mechanism of ER Stress and Inflammation for Hepatic Insulin Resistance in Obesity. *Ann Nutr Metab* 2015; **67**: 218-227 [PMID: [26452040](#) DOI: [10.1159/000440905](#)]
- 52 **Oyadomari S**, Harding HP, Zhang Y, Oyadomari M, Ron D. Dephosphorylation of translation initiation factor 2alpha enhances glucose tolerance and attenuates hepatosteatosis in mice. *Cell Metab* 2008; **7**: 520-532 [PMID: [18522833](#) DOI: [10.1016/j.cmet.2008.04.011](#)]
- 53 **Schwabe RF**, Uchinami H, Qian T, Bennett BL, Lemasters JJ, Brenner DA. Differential requirement for c-Jun NH2-terminal kinase in TNFalpha- and Fas-mediated apoptosis in hepatocytes. *FASEB J* 2004; **18**: 720-722 [PMID: [14766793](#) DOI: [10.1096/fj.03-0771fje](#)]
- 54 **Chen Y**, Brandizzi F. IRE1: ER stress sensor and cell fate executor. *Trends Cell Biol* 2013; **23**: 547-555 [PMID: [23880584](#) DOI: [10.1016/j.tcb.2013.06.005](#)]
- 55 **Guan BJ**, Krokowski D, Majumder M, Schmotzer CL, Kimball SR, Merrick WC, Koromilas AE, Hatzoglou M. Translational control during endoplasmic reticulum stress beyond phosphorylation of the translation initiation factor eIF2α. *J Biol Chem* 2014; **289**: 12593-12611 [PMID: [24648524](#) DOI: [10.1074/jbc.M113.543215](#)]
- 56 **Choi WG**, Han J, Kim JH, Kim MJ, Park JW, Song B, Cha HJ, Choi HS, Chung HT, Lee IK, Park TS, Hatzoglou M, Choi HS, Yoo HJ, Kaufman RJ, Back SH. eIF2α phosphorylation is required to prevent hepatocyte death and liver fibrosis in mice challenged with a high fructose diet. *Nutr Metab (Lond)* 2017; **14**: 48 [PMID: [28781602](#) DOI: [10.1186/s12986-017-0202-6](#)]
- 57 **Chao CY**, Battat R, Al Khoury A, Restellini S, Sebastiani G, Bessisow T. Co-existence of non-alcoholic fatty liver disease and inflammatory bowel disease: A review article. *World J Gastroenterol* 2016; **22**: 7727-7734 [PMID: [27678354](#) DOI: [10.3748/wjg.v22.i34.7727](#)]
- 58 **Gisbert JP**, Luna M, González-Lama Y, Pousa ID, Velasco M, Moreno-Otero R, Maté J. Liver injury in inflammatory bowel disease: long-term follow-up study of 786 patients. *Inflamm Bowel Dis* 2007; **13**: 1106-1114 [PMID: [17455203](#) DOI: [10.1002/ibd.20160](#)]
- 59 **Bargiggia S**, Maconi G, Elli M, Molteni P, Ardizzone S, Parente F, Todaro I, Greco S, Manzionna G, Bianchi Porro G. Sonographic prevalence of liver steatosis and biliary tract stones in patients with inflammatory bowel disease: study of 511 subjects at a single center. *J Clin Gastroenterol* 2003; **36**: 417-420 [PMID: [12702985](#)]
- 60 **Riegler G**, D'Inca R, Sturniolo GC, Corrao G, Del Vecchio Blanco C, Di Leo V, Carratù R, Ingresso M, Pelli MA, Morini S, Valpiani D, Cantarini D, Usai P, Papi C, Caprilli R. Hepatobiliary alterations in patients with inflammatory bowel disease: a multicenter study. Caprilli amp; Gruppo Italiano Studio Colon-Retto. *Scand J Gastroenterol* 1998; **33**: 93-98 [PMID: [9489915](#)]
- 61 **Bessisow T**, Le NH, Rollet K, Afif W, Bitton A, Sebastiani G. Incidence and Predictors of Nonalcoholic Fatty Liver Disease by Serum Biomarkers in Patients with Inflammatory Bowel Disease. *Inflamm Bowel Dis* 2016; **22**: 1937-1944 [PMID: [27379445](#) DOI: [10.1097/MIB.0000000000000832](#)]
- 62 **Jiang W**, Wu N, Wang X, Chi Y, Zhang Y, Qiu X, Hu Y, Li J, Liu Y. Dysbiosis gut microbiota associated with inflammation and impaired mucosal immune function in intestine of humans with non-alcoholic fatty liver disease. *Sci Rep* 2015; **5**: 8096 [PMID: [25644696](#) DOI: [10.1038/srep08096](#)]
- 63 **Da Silva HE**, Teterina A, Comelli EM, Taibi A, Arendt BM, Fischer SE, Lou W, Allard JP. Nonalcoholic fatty liver disease is associated with dysbiosis independent of body mass index and insulin resistance. *Sci Rep* 2018; **8**: 1466 [PMID: [29362454](#) DOI: [10.1038/s41598-018-19753-9](#)]
- 64 **Mouzaki M**, Comelli EM, Arendt BM, Bonengel J, Fung SK, Fischer SE, McGilvray ID, Allard JP. Intestinal microbiota in patients with nonalcoholic fatty liver disease. *Hepatology* 2013; **58**: 120-127 [PMID: [23401313](#) DOI: [10.1002/hep.26319](#)]
- 65 **Del Chierico F**, Nobili V, Vernocchi P, Russo A, Stefanis C, Gnani D, Furlanello C, Zandonà A, Paci P, Capuani G, Dallapiccola B, Miccheli A, Alisi A, Putignani L. Gut microbiota profiling of pediatric nonalcoholic fatty liver disease and obese patients unveiled by an integrated meta-omics-based approach. *Hepatology* 2017; **65**: 451-464 [PMID: [27028797](#) DOI: [10.1002/hep.28572](#)]
- 66 **Brahe LK**, Le Chatelier E, Prifti E, Pons N, Kennedy S, Hansen T, Pedersen O, Astrup A, Ehrlich SD, Larsen LH. Specific gut microbiota features and metabolic markers in postmenopausal women with obesity. *Nutr Diabetes* 2015; **5**: e159 [PMID: [26075636](#) DOI: [10.1038/nutd.2015.9](#)]
- 67 **Mouzaki M**, Wang AY, Bandsma R, Comelli EM, Arendt BM, Zhang L, Fung S, Fischer SE, McGilvray IG, Allard JP. Bile Acids and Dysbiosis in Non-Alcoholic Fatty Liver Disease. *PLoS One* 2016; **11**: e0151829 [PMID: [27203081](#) DOI: [10.1371/journal.pone.0151829](#)]
- 68 **Nobili V**, Putignani L, Mosca A, Chierico FD, Vernocchi P, Alisi A, Stronati L, Cucchiara S, Toscano M, Drago L. Bifidobacteria and lactobacilli in the gut microbiome of children with non-alcoholic fatty liver disease: which strains act as health players? *Arch Med Sci* 2018; **14**: 81-87 [PMID: [29379536](#) DOI: [10.5114/aoms.2016.62150](#)]



Published By Baishideng Publishing Group Inc  
7041 Koll Center Parkway, Suite 160, Pleasanton, CA 94566, USA  
Telephone: +1-925-2238242  
Fax: +1-925-2238243  
E-mail: [bpgoffice@wjgnet.com](mailto:bpgoffice@wjgnet.com)  
Help Desk: <https://www.f6publishing.com/helpdesk>  
<https://www.wjgnet.com>

